Article

Biobased Chemicals from D-Galactose: An Efficient Route to 5-Hydroxymethylfurfural Using a Water/MIBK System in Combination with an HCl/AlCl₃ Catalyst

Angela Martina, Henk H. van de Bovenkamp, Jozef G. M. Winkelman, Inge W. Noordergraaf, Francesco Picchioni, and Hero J. Heeres*

Read Online

ACCESS | ⭳ Metrics & More | 📄 Article Recommendations | 🆂🅸 Supporting Information

ABSTRACT: 5-Hydroxymethylfurfural (HMF) is an attractive building block for biobased chemicals. Typically, ketoses like D-fructose (FRC) are suitable starting materials and give good yields of HMF in a simple aqueous phase process with a Brønsted acid catalyst. With aldoses, such as D-glucose (GLU), much lower yields were reported in the literature. Here, we report an experimental and modeling study on the use of D-galactose (GAL) for HMF synthesis, using a liquid−liquid system (water/MIBK) in combination with an HCl/AlCl₃ catalyst. Experiments were conducted in a batch system with temperatures between 112 and 153 °C, HCl and AlCl₃ concentrations ranging from 0.02 to 0.04 M, and initial GAL concentrations between 0.1 and 1.0 M. The highest HMF yield was 49 mol % obtained for a batch time of 90 min at 135 °C. This value is much higher than in experiments with GAL in a monophasic aqueous system with HCl as the catalyst (2 mol % HMF yield) under similar reaction conditions. Based on detailed product analyses, a reaction scheme is proposed in which the isomerization of GAL to tagatose (TAG), catalyzed by the Lewis acid AlCl₃, is the first and key step. TAG is then converted to HMF by Brønsted acid HCl. The experimental data were modeled using a statistical approach as well as a kinetic approach. The kinetic model demonstrates a good agreement between the experimental and modeled data. Our findings reveal that temperature is the reaction variable with the most significant influence on the HMF yield. The use of a biphasic system appears to be a promising method for HMF production from GAL.
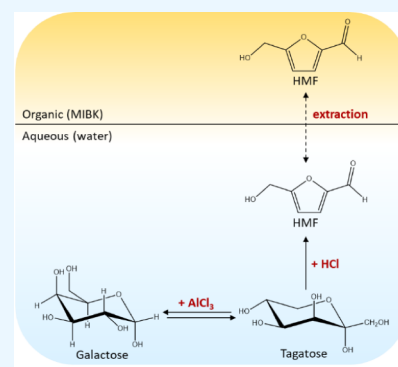
1. INTRODUCTION

Greenhouse gas emissions and global climate change issues have encouraged research on the use of sustainable resources for producing fuels and chemicals. Marine biomass like macroalgae or seaweed is an attractive feedstock due to its high growth rate, high carbohydrate content, and low lignin content.[1] When considering the production of biobased chemicals from marine biomass, HMF is an attractive target since it is a valuable and promising platform chemical. It offers ample opportunities for derivatization to obtain polymer precursors like 2,5-furandicarboxylic acid (FDCA) as well as to produce other valuable chemicals like formic acid (FA), 2,5-dimethyl furan, and levulinic acid (LA).[2,3]

In the last decades, various monomeric sugars have been investigated for HMF synthesis, especially glucose (GLU) and fructose (FRC). Although GLU is the most abundant monosaccharide that can be obtained from natural sources, it is not the most suitable monosaccharide for HMF synthesis. For instance, in aqueous systems with inorganic acids as catalysts, the HMF yield is very limited. This may be improved when using specific organic solvents (e.g., DMSO) though this often leads to expensive workup procedures to purify HMF.[2,4] In contrast, the use of FRC is more promising, and much higher yields are possible. Comprehensive reviews on utilizing GLU and FRC for

HMF synthesis have been published in recent years including HMF yield data and kinetics when using homogeneous (i.e., sulfuric acid, hydrochloric acid, phosphoric acid) and heterogeneous (i.e., NbOPO₄, acidic ion-exchange resins) catalysts, either in monophasic (i.e., water, organic solvents, ionic liquids, deep eutectic solvents) or biphasic systems (i.e., water/MIBK, water/acetone, water/THF), are available.[2,5,6]

Red seaweed is an interesting marine biomass that contains significant amounts of polysaccharides. One of the main building blocks is D-galactose (GAL). It is well-known that an aldose like GAL is, like GLU, less attractive for HMF synthesis as it gives low HMF yields (<10 mol %), particularly when using a simple reaction system consisting of water and an inorganic acid (Table 1). Yield improvements are possible by replacing water with an organic solvent and using aluminum salts as the catalyst. For instance, Jia and coworkers reported a maximum HMF yield of

Table 1. Overview of HMF and LA Syntheses from Macroalgae and Macroalgae-Derived Sugars

no.	feedstock	catalyst	solvent	maximum yields	ref.
	macroalgae				
1	*Gelidium amansii*	H_2SO_4	water	$C_{HMF} = 4.49$ g/L $C_{LA} = 11.45$ g/L	14
2	*Kappaphycus alvarezii*	H_2SO_4, HCl	water	$C_{HMF} = 4.85$ g/L $C_{LA} = 2.8$ g/L	15
3	*Gelidium latifolium*	H_2SO_4, HCl	water	$C_{HMF} = 5.7 \pm 0.48$ g/L $C_{LA} = 2.56 \pm 0.08$ g/L	16
4	*Gracilaria verrucosa*	H_2SO_4	water	$Y_{HMF} = 5.98$ wt % (3.74 g/L) $Y_{LA} = 18.64$ wt % (14.65 g/L)	17
5	*Kappaphycus alvarezii*	H_2SO_4	water	$C_{HMF} = 4.61$ g/L $C_{LA} = 12.42$ g/L	18
6	*Gelidium amansii*	[Tri-EG-(MIm)$_2$] 2HSO$_4$	[Tri-EG-(MIm)$_2$] 2HSO$_4$	$Y_{HMF} = 28.75 \pm 0.01$ mg/g	19
7	*Gracilaria verrucosa*	methanesulfonic acid	water	$Y_{HMF} = 7.04$ wt % $Y_{LA} = 23.61$ wt %	20
8	*Glacilaria fisheriGlaciaria tenuistipitata*	H_2SO_4	water	$C_{HMF} = 1.55$ g/L (*G. fisheri*)$C_{HMF} = 1.42$ g/L (*G. tenuistipitata*) $C_{LA} = 3.66$ g/L (*G. fisheri*)$C_{LA} = 6.12$ g/L (*G. tenuistipitata*)	21
9	*Ulva lactuca*	$ZnCl_2 \cdot nH_2O$/HCl	zinc chloride hydrate	$Y_{HMF} = 25$ mol %	22
10	*Ulva lactuca*	ChCl/oxalic acid	ChCl/oxalic acid/MIBK	$Y_{HMF} = 7$ mol %	23
11	*Enteromorpha prolifera*	$FeCl_3$	H_2O/THF/NaCl	$Y_{HMF} = 20.0$ wt %	24
12	*Ulva prolifera*	formic acid	H_2O/THF/NaCl	$Y_{HMF} = 10.6$ wt %	25
13	*Ulva lactuca*	H_2SO_4	water	$Y_{HMF} = 46.6$ g/kg (*Ulva lactuca*)	26
	polysaccharide				
14	κ-carrageenan	H_2SO_4, Mg(HSO$_4$)$_2$, HCl	water	$Y_{HMF} = 52.6\%$ $Y_{LA} = 82.4\%$	27
15	κ-carrageenan	HCOOH, CF$_3$COOH, HNO$_3$, HCl	water	$C_{HMF} = 5.03$ g/L $C_{LA} = 3.90$ g/L	28
16	κ-carrageenan	H_2SO_4	water	$Y_{HMF} = 18.4$ mol % $Y_{LA} = 29.7$ mol %	29
17	κ-carrageenan	self-catalyst DIC$_A$T-1	water	$Y_{HMF} = 50$ mol %	30
18	agarose	H_2SO_4, metal chloride (NaCl, CaCl$_2$, MgCl$_2$, ZnCl$_2$, CrCl$_3$, CuCl$_2$, and FeCl$_3$)	water	$Y_{HMF} = 40.7$ mol %	31
19	agarose	Amberlyst 36	DMSO	$Y_{HMF} = 62$ mol % (batch, DMSO)$Y_{LA} = 50$ mol % (batch, water)	32
20	agarose	No catalystH_2SO_4MgCl$_2$	water	$Y_{HMF} = 57$ mol %$Y_{LA} = $ max 64 mol %	33
	monosaccharide				
21	GAL	Lewatit SPC-108	water/MIBK	$Y_{HMF} = 5$ mol %	9
22	GAL	LaCl$_3$	DMSO	$Y_{HMF} = 6.7\%$	34
23	GAL	H_2SO_4, CrCl$_2$, CrCl$_3$, CrBr$_3$, Cr(NO$_3$)$_3$Additives: LiCl, LiBr	[EMIM]Cl, DMA, DMSO	$Y_{HMF} = 1$–33mol %	35
24	GAL	HT, Amberlyst-15	DMF	$Y_{HMF} = 21.3\%$	36
25	GAL	Amberlyst-70	ethanol/water	$Y_{HMF} = 3$ mol %	37
26	GAL	[NMP][HSO$_4$] [NMP][HSO$_4$] [C$_3$SO$_3$HMIM][HSO$_4$] [C$_3$SO$_3$HMIM][HSO$_4$] Additive: CoCl$_2$	[AMIM]Cl [BMIM]Cl	$Y_{HMF} = 19.7$ mol %	38
27	GAL	H_2SO_4	water	$Y_{HMF} = 2.5$ mol %	39
28	GAL	AlCl$_3 \cdot 6H_2O$	DMSO/water	$Y_{HMF} = 34.6$ mol %	7

34.6 mol % in DMSO/water mixtures using $AlCl_3 \cdot 6H_2O$ as the catalyst at 130 °C.[7]

Further improvement of the HMF yield with aldoses like GLU as the feed is possible by using a biphasic liquid−liquid system. Here, the idea is to prevent further reactions of HMF by extracting it from the water phase to an organic phase such as methyltetrahydrofuran (MTHF), or methyl isobutyl ketone (MIBK). The latter is the preferred one since it is cheap, has low toxicity, and has a high HMF partition coefficient in a mixture with water compared to other common organic solvents.[8]

Although biphasic systems in combination with suitable catalysts have successfully been applied for GLU as feedstock,[2,4] the conversion of GAL to HMF with such a system has not been reported to date. The only exception is research by Rigal et al. on the conversion of GAL in water/MIBK using a heterogeneous catalyst (Lewatit SPC-108). However, the highest HMF yield was only 5 mol % at 78 °C and 16 h reaction time in a batch reactor.[9]

In the present paper, we report the conversion of GAL to HMF using a biphasic system in combination with a combined Brønsted−Lewis acid catalyst ($HCl/AlCl_3$). This approach is inspired by recent work in our group using this system with GLU as the feed, giving a maximum HMF yield of 70 mol %.[10] These high yields were explained by assuming that GLU is initially isomerized to FRC by a Lewis acid such as Al^{3+}, followed by a Brønsted acid-catalyzed conversion of FRC to HMF.

The use of the combined Brønsted−Lewis acid catalyst ($HCl/AlCl_3$) for GAL conversion to HMF is motivated by assuming that GAL is known to be easily isomerized to tagatose (TAG) and talose (TAL) in the presence of a Lewis acid like $AlCl_3$. This isomerization step of GAL to TAG is considered essential, as, in contrast to GAL, TAG has been shown to be a much better precursor for HMF synthesis. HMF yields of up to 30 mol % have been reported (75 min batch time, 65 g·L^{-1} substrate concentration, 33 mM H_2SO_4 at 120 °C).[11]

Generally, the isomerization of GAL into TAG is conducted in the presence of either a base or a Lewis acid catalyst. However, base catalysts appear to be of low efficiency due to the coproduction of sorbose (SOR) and acidic byproducts.[12] The use of a Lewis acid has proven to be more effective, and a high selectivity of TAG without SOR formation was observed when using for example Sn-BEA.[12,13] An overview of typical isomerization catalysts for GAL to TAG is given in Table S1.

In the present work, the conversion of GAL to HMF has been investigated using an $HCl/AlCl_3$ mixture as the catalyst, in a biphasic system consisting of water and MIBK. The use of the hybrid catalyst is motivated by previous research in our group on GLU conversion to HMF showing that an isomerization reaction of GLU to FRC is key to obtain high HMF yields. The hybrid catalyst showed good performance in this respect.[10] It is anticipated that an initial isomerization of GAL to TAG is a key reaction in our system and, in analogy with the system above, is catalyzed by $HCl/AlCl_3$. MIBK was selected as the organic solvent as it is one of the best ones when considering HMF synthesis from aldohexoses like GLU.[2,4]

A total of 25 experiments were performed in a batch setup at temperatures between 112 and 153 °C, with different initial concentrations of GAL ($C_{GAL,0}$, 0.1−1 M) and $HCl/AlCl_3$ (C_{HCl} = C_{AlCl_3} = 0.02−0.08 M). The liquid phases after the reactions were analyzed using HPLC (for the aqueous phase) and GC (for the organic phase), and the concentrations of GAL, HMF, and byproducts were quantified. The concentration−time curves

were modeled using a statistical design of experiment (DOE) as well as a kinetic approach.

2. EXPERIMENTAL SECTION

2.1. Chemicals. All chemicals were used without further purification. D-Galactose (GAL, 99%) [CAS: 59−23−4] was purchased from Acros Organics. H_2SO_4 (95−97%) [7664−93−9] and HCl (37−38%) [7647−01−0] were purchased from Boom. D-Tagatose (TAG, ≥98.5%) [87−81−0], D-sorbose (SOR, ≥99%) [3615−56−3], D-talose (TAL, ≥99%) [2595−98−4], HMF (99%) [67−47−0], $AlCl_3 \cdot 6H_2O$ (99%) [7784−13−6], formic acid (FA, ≥95%) [64−18−6], and methyl isobutyl ketone (MIBK, ≥99.5%) [108−10−1] were obtained from Sigma-Aldrich. LA (98%) [123−76−2] was purchased from Alfa Aesar. Milli-Q water was used to prepare the solutions.

2.2. Experimental Procedures. The experimental procedures are based on a procedure given by Guo et al.[8,10] The experiments were conducted with temperatures between 112 and 153 °C, HCl and $AlCl_3$ concentrations between 0.02 and 0.08 M, and initial GAL concentrations between 0.1 and 1.0 M. In all cases, a 1 to 1 mol ratio of both catalyst components (HCl and $AlCl_3$) was applied.

The reactions were carried out in Ace pressure tubes (bushing type, front seal, with a volume of about 9 mL, L × O.D. 10.2 cm × 1.9 cm). The pressure tubes were filled with approximately 5 mL of the solution consisting of 1 mL of aqueous reactant solution (a mixture of GAL with $HCl/AlCl_3$) and 4 mL of MIBK. A poly(tetrafluoroethylene) (PTFE)-coated stirring bar was added to the tubes. The tubes were then closed with plug-sealed screw caps. A series of tubes were placed in an aluminum rack, and the rack was placed in an oil bath at a specified temperature and stirred at 900 rpm to avoid mass transfer limitations. At certain times, a tube was taken from the oil bath and directly quenched in a cold-water bath to stop the reaction. The tubes were stored at room temperature for 2 h to ensure the equilibrium partitioning of the various products between both liquid phases. Then, the tubes were opened, and the aqueous phase and organic phase were filtered using a PTFE syringe filter (0.45 μm) before being analyzed by HPLC and GC, respectively. The reproducibility of the experiments was tested by conducting several duplicate experiments. The results are given in Figure S1 and reveal that the reproducibility of the experiments is good.

2.3. Analytical Methods. The aqueous phase composition was determined using an Agilent 1200 HPLC system equipped with an Agilent 1200 pump, a Bio-Rad organic acid column (Aminex HPX-87H), a refractive index detector, and an ultraviolet detector. An aqueous sulfuric acid (5 mM) solution was used as the mobile phase at a flow rate of 0.55 mL min^{-1}. The HPLC column was operated at 60 °C. The analysis for a sample was completed in 45 min.

The organic phase was analyzed by an Agilent 8860 GC, equipped with a flame ionization detector (FID) operated at 260 °C and a Stabilwax-DA column (length: 30 m; diameter: 320 μm; film thickness: 1 μm). One μL portion of the sample was injected, and a split ratio of 1:50 and an inlet temperature of 260 °C were applied. Helium was used as the carrier gas at a flow rate of 3 mL/min. The oven temperature was initially set at 40 °C and maintained at this temperature for 5 min, then increased to 240 °C (15 °C/min), and held at 240 °C for 10 min. The concentration of each compound in the aqueous and organic samples was calculated by using calibration curves obtained by analyzing standard solutions with known concentrations.

2.4. Definitions and Calculations of the Conversion and Yield. The conversion of substrate (X_s) and yield of products (Y_p) were calculated by using eqs 1 and 2.

$$X_s = \frac{V_{aq,0}C_{aq,s,0} - V_{aq,1}C_{aq,p,1}}{V_{aq,0}C_{aq,s,0}} \times 100\% \tag{1}$$

$$Y_p = \frac{V_{org,1}C_{org,p,1} + V_{aq,1}C_{aq,p,1}}{V_{aq,0}C_{aq,s,0}} \times 100\% \tag{2}$$

Due to the partial miscibility of water and MIBK, $V_{aq,1}$ and $V_{org,1}$ differ from $V_{aq,0}$ and $V_{org,0}$, respectively, and were corrected using eqs 3 and 4.

$$V_{aq,1} = V_{aq,0}\alpha_{aq} \tag{3}$$

$$V_{org,1} = V_{org,0}\alpha_{org} \tag{4}$$

Here, α_{aq} and α_{org} are correction factors, and these were calculated using Aspen software (Table S3).

2.5. Statistical Analyses. The yield of HMF (eq 2) was optimized by a design of experiment (DOE) method, wherein the temperature, HCl/AlCl$_3$ concentration, and initial GAL concentration were considered as the independent variables. The process was optimized using Design-Expert 7 software, and the HMF yield was modeled using a standard expression, as given in eq 5.

$$Y_{HMF} = b_0 + \sum_{i=1}^{3} b_i x_i + \sum_{i=1}^{3}\sum_{j=1}^{3} b_{ij} x_i x_j \tag{5}$$

The effects of the process variables x_i (temperature, HCl and AlCl$_3$ concentration, and initial GAL concentration), indicated as indices 1−3, on the HMF yield were modeled, and the regression coefficients were determined. The significance of these factors was assessed using the p-value in the ANOVA analysis. A factor was considered statistically relevant if the p-value was lower than 0.05. Backward elimination regression was performed based on diagnostic assessments to improve the model.

3. RESULT AND DISCUSSION

3.1. General Considerations. A total of 25 experiments were performed in the temperature range of 112−153 °C with different initial concentrations of GAL ($C_{GAL,0}$, 0.1−1 M), and HCl/AlCl$_3$ ($C_{HCl} = C_{AlCl_3} = 0.02−0.08$ M), see Table 2 for

Table 2. Reaction Conditions for HMF Synthesis from GAL in Water/MIBK System

parameter	value	benchmark conditions	conditions for $Y_{HMF,max}$
temperature, T (°C)	112−153	143	135
concentration of HCl and AlCl$_3$ (M)	0.02−0.08	0.04	0.08
initial GAL concentration, $C_{GAL,0}$ (M)	0.1−1	0.1	0.1

details. All experiments reported in this study were conducted in a batch reactor setup, and liquid samples were taken at regular time intervals and analyzed. In all cases, a 1 to 1 mol ratio of both catalyst components (HCl and AlCl$_3$) was applied. This ratio is based on optimization studies using this hybrid catalyst system

for GLU isomerization to FRC,[10] and we anticipated that the same holds for the related GAL to TAG isomerization reaction.

A typical concentration−time curve for a representative batch experiment ($C_{GAL,0}$: 0.1 M, $C_{HCl} = C_{AlCl_3} = 0.08$ M, 135 °C) is given in Figure 1. The GAL concentration drops over time, and
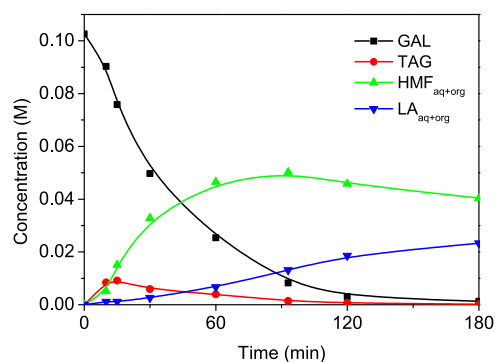

Figure 1. Typical concentration profile of the conversion of GAL to HMF in water/MIBK in the presence of HCl/AlCl$_3$. Conditions: $C_{GAL,0}$ = 0.1 M; $C_{HCl} = C_{AlCl_3} = 0.08$ M; 135 °C. Symbols: measured data; lines: trend line.

quantitative conversion is obtained after about 120 min. TAG and HMF show a maximum concentration and are thus clearly intermediates in the reaction network. The main byproduct that could be detected with HPLC is LA, which is known to be formed by a subsequent reaction of HMF. Additionally, some other byproducts including TAL and FA are present. TAL is a known side product of GAL isomerization to TAG in the presence of a Lewis acid (in this case AlCl$_3$),[12,13] whereas FA is a side product from the further rehydration of HMF to LA in the presence of HCl. Finally, insoluble byproducts in the form of brown solids, also known as humins, are formed. These were difficult to isolate and could not be quantified. A representative carbon balance versus batch time is given in Figure S2. It clearly shows that the amount of detectable compounds (HPLC/GC) is reduced upon prolonged batch times, and this is likely due to the formation of such initially soluble and later insoluble humins. Based on the experimental data, a simplified reaction network is proposed and given in Scheme 1.

By using this catalyst system in combination with the process conditions given above, the HMF yield peaked at 49 mol % for a batch reaction time of about 90 min. This is considerably higher than when using a simple monophasic reaction system consisting of water and an inorganic acid (Table 1, <10 mol %). This result clearly demonstrates that high HMF yields are also possible when using GAL as the feed, providing that a suitable catalyst and a biphasic liquid−liquid system are used.

To gain insights into the role of the two catalyst components in the reaction network, additional experiments were performed with the individual catalyst components. The results of these experiments, in the form of the conversion of GAL, yield of TAG, and yield of HMF as a function of batch reaction time, are given in Figure 2. The conversion of GAL is strongly dependent on the catalyst used. The best result was obtained with AlCl$_3$ only, with quantitative conversion after 90 min. The reaction with AlCl$_3$ in combination with HCl is slower, and almost a quantitative conversion is obtained after 120 min. Under these conditions, HCl alone is by far less active, and the maximum conversion was only 20 mol % after 120 min batch time. The HMF yields (Figure 2c) are also substantially higher with the
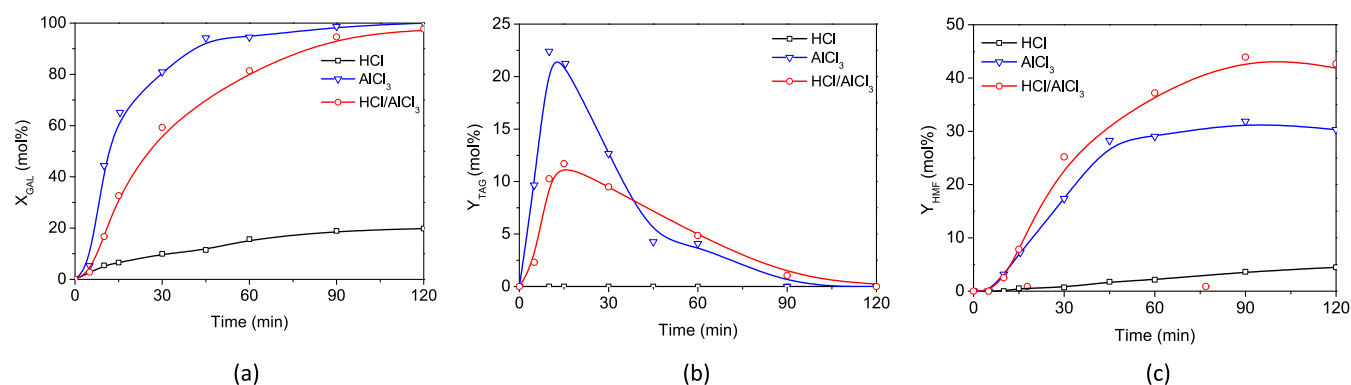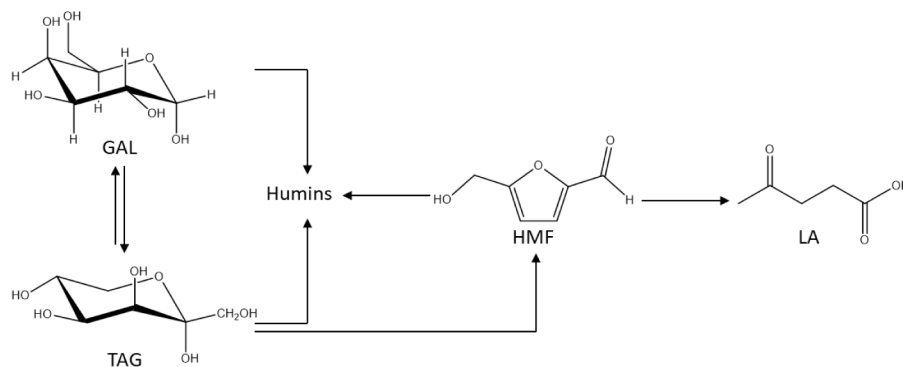
Scheme 1. Simplified Reaction Network for the Conversion of GAL to HMF with the Hybrid HCl/AlCl$_3$ Catalyst

Figure 2. Conversion of GAL (a), yield of TAG (b), and yield of HMF (c) versus batch time using HCl, AlCl$_3$, and HCl/AlCl$_3$ catalysts in water/MIBK. Conditions: 143 °C; C_{acid} = 0.04 M; $C_{GAL,0}$ = 0.1 M. Symbols: measured data; lines: trend line.
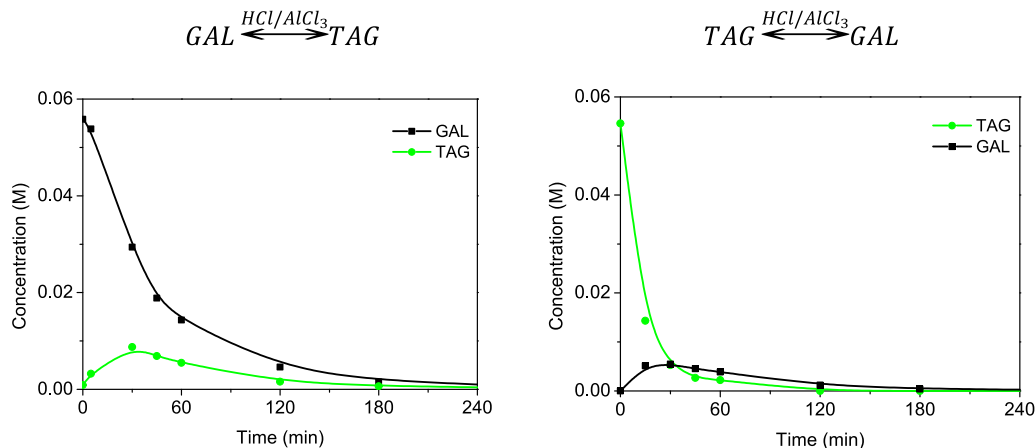
$$GAL \underset{}{\overset{HCl/AlCl_3}{\rightleftarrows}} TAG \qquad\qquad TAG \underset{}{\overset{HCl/AlCl_3}{\rightleftarrows}} GAL$$

Figure 3. GAL isomerization to TAG (left) and conversion of TAG to GAL (right). Conditions: 140 °C; C_{HCl} = C_{AlCl_3} = = 0.04 M; $C_{sugars,0}$ = 0.05 M. Symbols: measured data; lines: trend line.

AlCl$_3$-based catalyst systems and at least a factor of 5 higher than that for HCl alone. The yields of HMF are higher when using the HCl/AlCl$_3$ system (44 mol % max) instead of AlCl$_3$ alone.

An explanation for these differences in HMF yields for the three catalyst systems is apparent when considering the TAG yield versus batch time. When using AlCl$_3$ in the catalyst system, significant amounts of TAG are formed, indicating that AlCl$_3$ is an active catalyst for the desired isomerization of GAL to TAG. Although aluminum salts have not been tested for this specific isomerization, other Lewis acids are known to catalyze the isomerization of GAL to TAG.[7,12,40] TAG was not identified when HCl was used in the absence of AlCl$_3$, implying that the Brønsted acid is not active for the isomerization step. TAG is

clearly the intermediate in the reaction network, and the batch profiles indicate that it is the precursor for HMF. The HMF yields are higher for the combination HCl/AlCl$_3$ than for AlCl$_3$ alone. Apparently, the conversion of TAG to HMF is facilitated by the action of the Brønsted acid HCl, as can be concluded from the profiles in Figure 2b,c.

Additional experiments were performed with TAG as the feed in combination with HCl and AlCl$_3$ to further prove that TAG and GAL are easily interconverted within the time scale of the reactions reported in this study. The results are given in Figure 3 and clearly show that when using TAG as the feed, GAL is formed, though in minor amounts, as further reactions to, for example, HMF prevail.
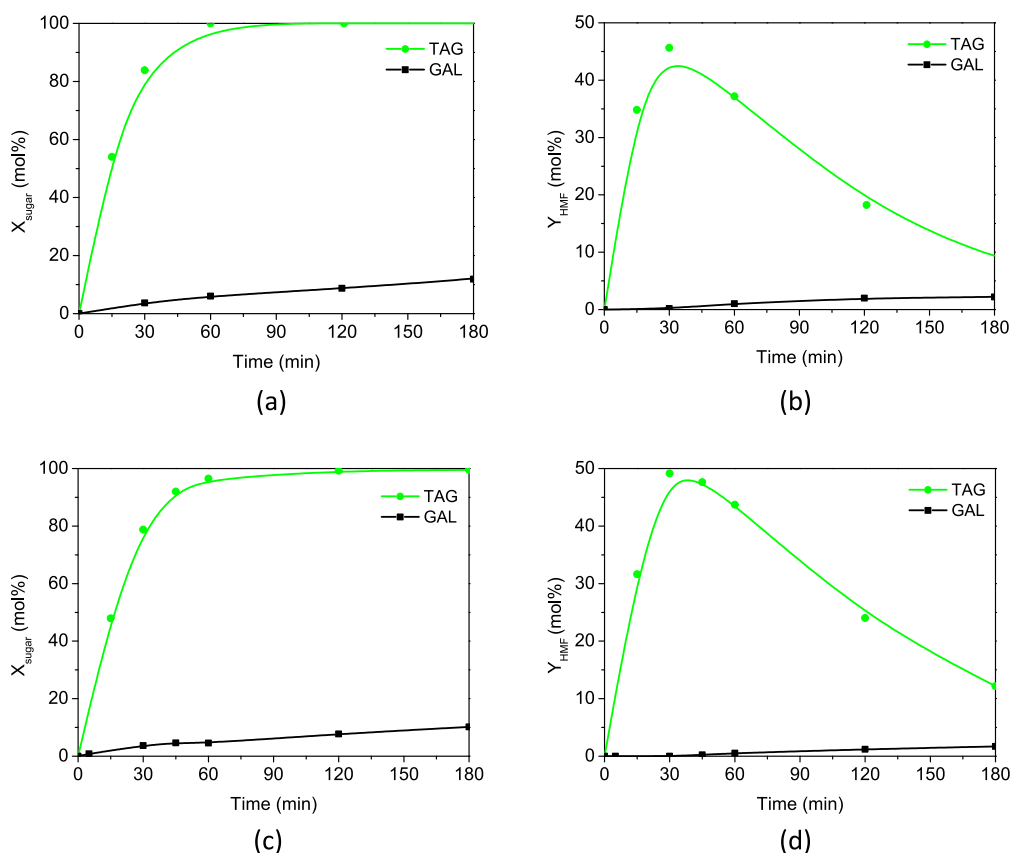
Figure 4. Comparison of the GAL and TAG conversions to HMF in water. Conditions: $T = 140\ ^\circ\text{C}$, $C_{\text{sugar},0} = 0.055\ \text{M}$, $C_{\text{H}_2\text{SO}_4} = 0.05\ \text{M}$ (a and b); $C_{\text{HCl}} = 0.04\ \text{M}$ (c and d). Symbols: measured data; lines: trend line.

The assumption that HMF is preferentially formed from TAG and not from GAL was further strengthened by performing Brønsted acid-catalyzed reactions (H_2SO_4 and HCl) of GAL and TAG with respect to HMF in water. Figure 4 shows that the conversion rate of TAG is much faster than for GAL. It requires 60−120 min to achieve quantitative conversion of TAG, while even after 180 min of reaction, GAL conversion remains below 12 mol % (Figure 4a,c). Furthermore, a maximum of 49 mol % of HMF (Figure 4d) can be obtained from TAG, whereas GAL produces less than 3 mol % of HMF (Figure 4b). These results clearly indicate that (i) the initial conversion of GAL to TAG is a prerequisite for high HMF yield and that (ii) Brønsted catalysts effectively catalyze the conversion of TAG to HMF.

Thus, we can conclude that high HMF yields from GAL are possible using a combination of AlCl_3 and HCl, where Al salts catalyze the isomerization of GAL to TAG, followed by a Brønsted acid-catalyzed conversion of TAG to HMF.

3.2. Effect of Process Variables on the GAL Conversion and Yield of TAG and HMF. The effect of the temperature, the concentration of the catalyst (HCl/AlCl_3), and the initial concentration of GAL were investigated to identify the process conditions that give the highest yields of HMF. The results are summarized in Table 3.

HMF yields within the experimental window ranged from 2.7 to 48.9 mol %. The best results were obtained at a batch time of 90 min at 135 °C, $C_{\text{GAL},0} = 0.1\ \text{M}$, and $C_{\text{HCl}} = C_{\text{AlCl}_3} = 0.08\ \text{M}$.

3.2.1. Effect of Temperature on HMF Yield. Temperature has a profound effect on the conversion of GAL. This is illustrated in Figure 5, which shows the batch profiles at a range of temperatures, while the other conditions were set at the

Table 3. Overview of Experiments for GAL Conversion to HMF in Water/MIBK

no.	$C_{\text{GAL},0}$ (M)	$C_{\text{HCl}} = C_{\text{AlCl}_3}$ (M)	T (°C)	$Y_{\text{HMF,max}}$ (mol %)
1	0.1	0.02	112	2.7
2	0.1	0.02	143	45.9
3	0.1	0.02	153	45.0
4	0.5	0.02	127	29.5
5	1	0.02	112	4.0
6	1	0.02	143	37.9
7	1	0.02	153	39.0
8	0.1	0.04	112	4.7
9	0.1	0.04	127	30.4
10	0.1	0.04	135	41.1
11	0.1	0.04	143	43.9
12	0.1	0.04	153	45.5
13	0.5	0.04	127	32.3
14	0.5	0.04	135	38.3
15	0.5	0.04	143	40.0
16	1	0.04	112	8.0
17	1	0.04	127	26.7
18	1	0.04	135	38.1
19	1	0.04	143	37.5
20	0.1	0.08	112	6.8
21	0.1	0.08	135	48.9
22	0.1	0.08	153	46.7
23	0.5	0.08	127	30.8
24	1	0.08	112	6.7
25	1	0.08	143	34.9

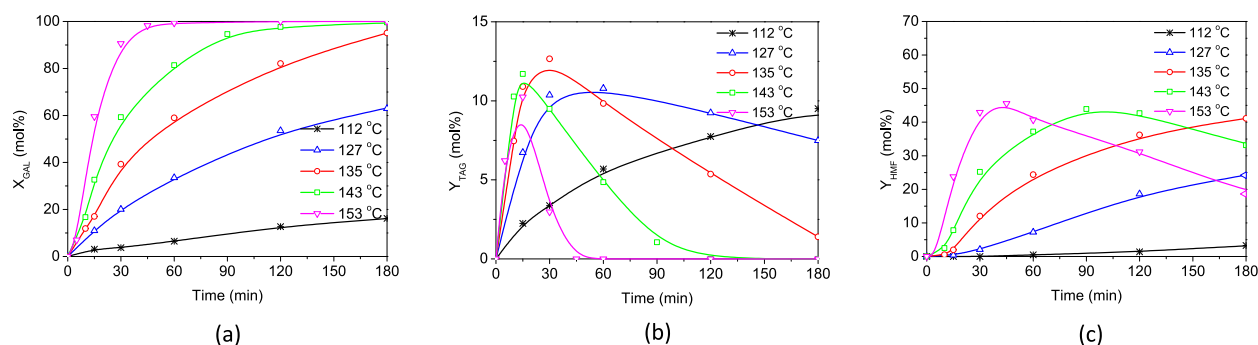**Figure 5.** Conversion of GAL (a), yield of TAG (b), and yield of HMF (c) versus batch time at different temperatures. Conditions: $C_{HCl} = C_{AlCl_3} = 0.04$ M; $C_{GAL,0} = 0.1$ M. Symbols: measured data; lines: trend line.
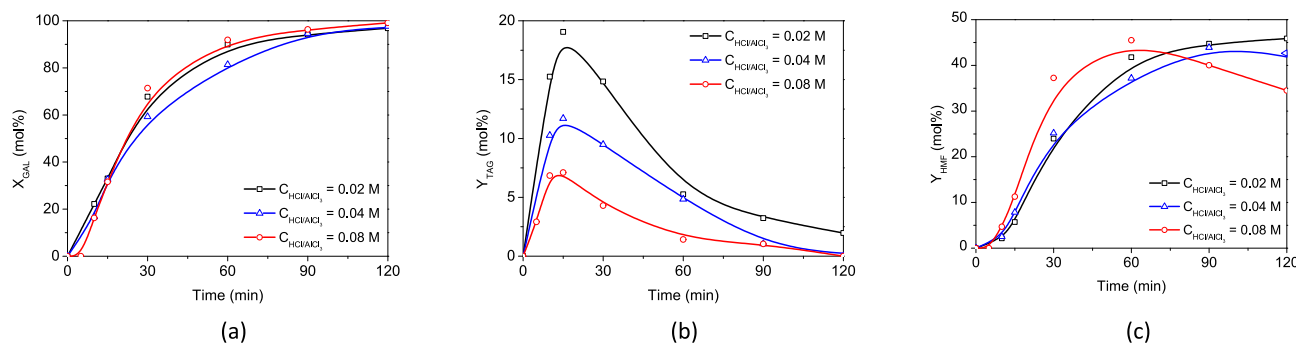

Figure 6. Conversion of GAL (a), yield of TAG (b), and yield of HMF (c) versus batch time at different concentrations of HCl/AlCl$_3$ (fixed 1 to 1 molar ratio). Conditions: $T = 143$ °C, $C_{GAL,0} = 0.1$ M. Symbols: measured data; lines: trend line.
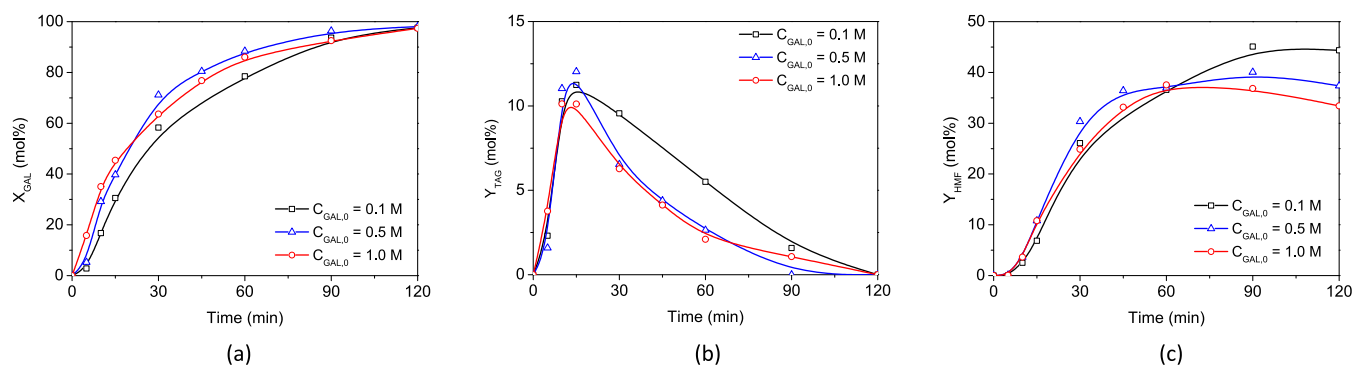

Figure 7. Conversion of GAL (a), yield of TAG (b), and yield of HMF (c) versus batch time at different initial concentrations of GAL. Conditions: $T = 143$ °C, $C_{HCl} = C_{AlCl_3} = 0.04$ M. Symbols: measured data; lines: trend line.

benchmark conditions (Table 2). At 153 °C, the highest temperature in the range, quantitative conversion of GAL was accomplished within 60 min, whereas at 112 °C, less than 20 mol % of GAL conversion was achieved after 180 min (Figure 5a). HMF yield is also temperature dependent, and at benchmark conditions, a maximum HMF yield of 46 mol % was reached after 45 min at 153 °C (Figure 5c).

3.2.2. Effect of HCl/AlCl$_3$ Concentration on HMF Yield. The concentration of HCl/AlCl$_3$ (fixed 1 to 1 molar ratio) does not have a major effect on the GAL conversion rates (Figure 6a). A higher concentration of HCl/AlCl$_3$ leads to a decrease in the maximum achievable yield of TAG (Figure 6b). Furthermore, the maximum HMF yield is only marginally affected, though the rate of HMF formation is somewhat higher when the highest catalyst concentration in the range is used (Figure 6c).

3.2.3. Effect of Initial Concentration of GAL. The initial concentration of GAL has only a minor effect on GAL

conversion; see Figure 7a for details. This is an indication that the conversion of GAL is a first-order reaction in GAL. The maximum HMF yield, however, shows a clear dependence on the initial concentration, and lower initial concentrations of GAL result in higher HMF yields (Figure 7c).

3.3. Statistical Modeling to Identify the Optimum Process Conditions for High HMF Yield. The experimental data of the 25 experiments (Table 3) were analyzed by using Design-Expert software to quantify the effect of process conditions on HMF yields and to find the maximum yield within the range of reaction variables applied here. The best model is given in eq 6 and shows a good fit between the data and model ($R^2 = 0.9857$). This is also confirmed by a parity plot shown in Figure 8. The analysis of the variance of the model is given in Table 4.

$$Y_{HMF} = -(642.38) + (9.23)T + (90.43)C_{HCl/AlCl_3}$$
$$+ (41.28)C_{GAL,0} - (0.31)TC_{GAL,0}$$
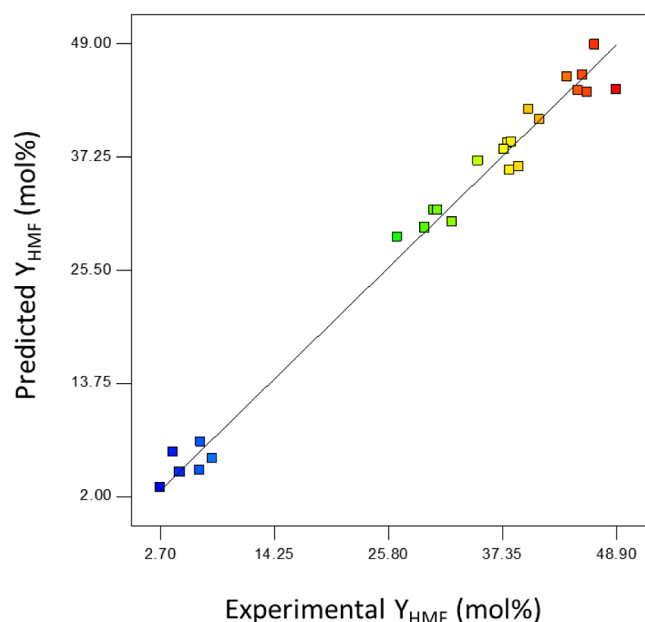$$- (120.99)C_{HCl/AlCl_3}C_{GAL,0} - (0.03)T^2 \quad (6)$$

Figure 8. Parity plot of the experimental Y_{HMF} and the predicted Y_{HMF} from the statistical model.

Table 4. Analysis of Variance of the Best Model

source	sum of square	degree of freedom	mean square	F-value	p-value prob > F
model	5680.58	6	946.76	206.44	<0.0001
T (A)	3428.95	1	3428.95	747.69	<0.0001
$C_{HCl/AlCl_3}$ (B)	6.50	1	6.50	1.42	0.2494
$C_{GAL,0}$ (C)	130.93	1	130.93	28.55	<0.0001
AC	88.81	1	88.81	19.37	0.0003
BC	28.44	1	28.44	6.20	0.0228
A^2	715.31	1	715.31	155.98	<0.0001
residual	82.55	18	4.59		

The statistical model shows that temperature has a significant effect on the yield of HMF, see Figure 9, left for details. Both the HCl/AlCl$_3$ concentration and initial GAL concentration have a minor impact on the HMF yields (Figure 9, right), also in line with the experimental data set.

3.4. Kinetic Modeling for GAL Conversion to HMF in Water/MIBK System. For reactor design purposes and process optimization, a kinetic model is more appropriate than the statistical model discussed above. Based on the experimental observations, a reaction network for the conversion of GAL to HMF in the biphasic system is proposed and is shown in Figure 10.

A kinetic model for the GAL conversion to HMF in the water MIBK-system was developed based on this reaction network and the following considerations:

1. GAL is in equilibrium with TAG, as shown experimentally in the previous section and supported by the literature data. Furthermore, it is assumed that TAG is the main precursor for

HMF formation since the rate of GAL directly to HMF is by far lower (see the General Considerations section).

2. The formation of dark-colored solids, commonly referred to as humins, is observed during most of the reactions. This is typical for acid-catalyzed conversions of sugars, such as FRC, GLU, GAL, and TAG, as well as HMF, and its formation is thus included in the reaction network.

3. The initial concentration of GAL has no significant impact on the conversion of GAL (Figure 7a). Similarly, the concentration of HCl/AlCl$_3$ also has a minor effect on the yield of HMF, which is also confirmed by the statistical model (Table 4). These observations suggest that the order in the reaction for GAL and the catalyst is close to 1. On the basis of these considerations, the reaction rates of the individual reactions in the network given in Figure 10 are defined as first-order reactions (eqs 7–13).

$$R_{1G} = k_{1G}C_{GAL} \quad (7)$$

$$R_{2G} = k_{2G}C_{GAL} \quad (8)$$

$$R_{1T} = k_{1T}C_{TAG} \quad (9)$$

$$R_{2T} = k_{2T}C_{TAG} \quad (10)$$

$$R_{3T} = k_{3T}C_{TAG} \quad (11)$$

$$R_{1H} = k_{1H}C_{HMF} \quad (12)$$

$$R_{2H} = k_{2H}C_{HMF} \quad (13)$$

4. The temperature dependence of the kinetic constants is introduced using modified Arrhenius equations (eqs 14–20). At the initial stage of the reaction, the reaction occurs in a nonisothermal way, due to the heating up of the tubes and their contents from room temperature to reaction temperature. To compensate this nonisothermal behavior in the kinetic modeling studies, the temperature inside the tubes as a function of the time during the heating-up stage was determined experimentally (Section S3).

$$k_{1G} = C_{HCl}k_{1RG}exp\left[\frac{E_{1G}}{R}\left(\frac{T-T_R}{T_R T}\right)\right] \quad (14)$$

$$k_{2G} = C_{AlCl_3}k_{2RG}exp\left[\frac{E_{2G}}{R}\left(\frac{T-T_R}{T_R T}\right)\right] \quad (15)$$

$$k_{1T} = C_{HCl}k_{1RT}exp\left[\frac{E_{1T}}{R}\left(\frac{T-T_R}{T_R T}\right)\right] \quad (16)$$

$$k_{2T} = C_{HCl}k_{2RT}exp\left[\frac{E_{2T}}{R}\left(\frac{T-T_R}{T_R T}\right)\right] \quad (17)$$

$$k_{3T} = C_{AlCl_3}k_{3RT}exp\left[\frac{E_{3T}}{R}\left(\frac{T-T_R}{T_R T}\right)\right] \quad (18)$$

$$k_{1H} = C_{HCl}k_{1RH}exp\left[\frac{E_{1H}}{R}\left(\frac{T-T_R}{T_R T}\right)\right] \quad (19)$$

$$k_{2H} = C_{HCl}k_{2RH}exp\left[\frac{E_{2H}}{R}\left(\frac{T-T_R}{T_R T}\right)\right] \quad (20)$$

5. Due to the partial miscibility between water and MIBK, the liquid volume of both phases changes after mixing and heating to the reaction temperature. Therefore, the actual volumes of two phases during the reaction need to be corrected (eqs 21 and 22). Here, the correction factors for the volume ratios (γ_{aq}, γ_{org}) have been calculated using Aspen Plus software (Table S4).
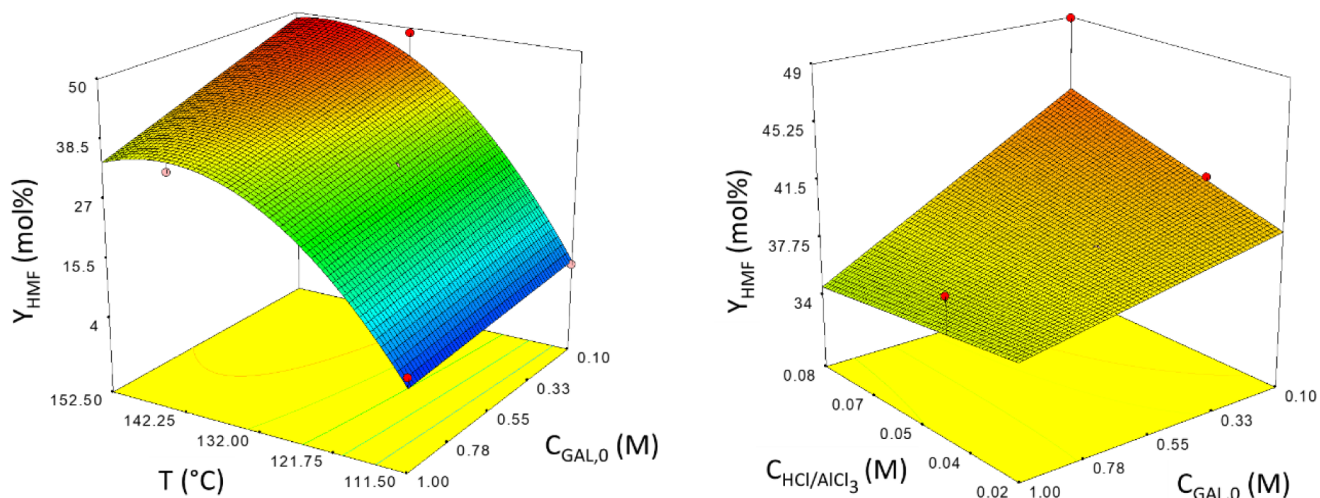
Figure 9. Modeled effects of temperature, HCl/AlCl$_3$ concentration, and initial concentration of GAL on the HMF yield. Conditions: $C_{HCl} = C_{AlCl_3} = 0.08$ M (left), and $T = 135$ °C (right).
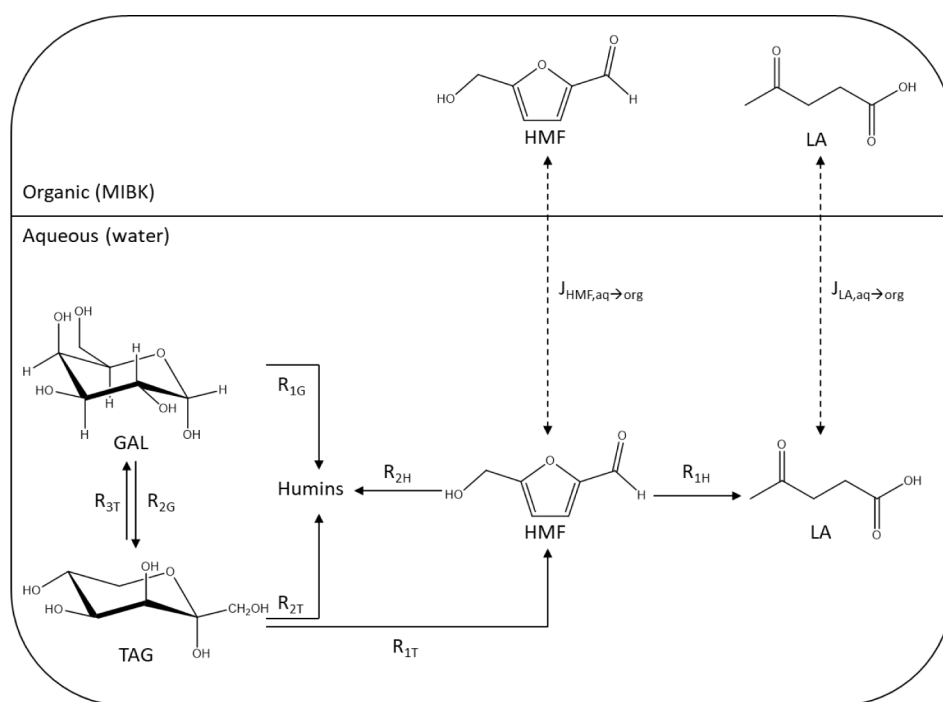

Figure 10. Proposed reaction network for the conversion of GAL to HMF in a biphasic (water/MIBK) system.

$$V_{aq,1} = V_{aq,0} \gamma_{aq} \tag{21}$$

$$V_{org,1} = V_{org,0} \gamma_{org} \tag{22}$$

The HCl and AlCl$_3$ concentrations are also corrected for these changes in the volume of both phases by using eqs 23 and 24.

$$C_{AlCl_3} = \frac{C_{AlCl_3,0}}{\gamma_{aq}} \tag{23}$$

$$C_{HCl} = \frac{C_{HCl,0}}{\gamma_{aq}} \tag{24}$$

6. A batch reactor model for both GAL and TAG is given in eqs 25 and 26. Here, it is assumed that the solubility of GAL and TAG in the organic phase is negligible.

$$\frac{dC_{GAL,aq}}{dt} = -R_{1G} - R_{2G} + R_{3T} \tag{25}$$

$$\frac{dC_{TAG,aq}}{dt} = -R_{1T} - R_{2T} - R_{3T} + R_{2G} \tag{26}$$

7. During the reaction, HMF and byproduct (LA) are transferred to the MIBK phase. When assuming that both do not react in the MIBK phase, the concentrations of HMF and LA in the water and organic phase (i.e., $C_{aq,HMF}$, $C_{org,HMF}$, $C_{aq,LA}$, $C_{org,LA}$) may be calculated by the mole balances given in eqs 27–30:

$$\frac{dC_{HMF,aq}}{dt} = R_{1T} - R_{1H} - R_{2H} - (J_{HMF} \cdot A)_{HMF_{aq \to org}} \tag{27}$$

$$\frac{dC_{\text{HMF,org}}}{dt} = (J_{\text{HMF}} \cdot A)_{\text{HMF}_{\text{aq} \to \text{org}}} \tag{28}$$

$$\frac{dC_{\text{LA,aq}}}{dt} = R_{1\text{H}} - (J_{\text{LA}} \cdot A)_{\text{LA}_{\text{aq} \to \text{org}}} \tag{29}$$

$$\frac{dC_{\text{LA,org}}}{dt} = (J_{\text{LA}} \cdot A)_{\text{LA}_{\text{aq} \to \text{org}}} \tag{30}$$

Here, A is the interfacial area between the water and organic phases, and J_i is the molar mass transfer rate of component i per unit surface area (i.e., HMF, LA). When the film model is assumed to be valid, the molar mass transfer rates are provided in eqs 31 and 32:

$$J_i = k_{\text{L,aq}}(C_{i,\text{aq}} - C_{i,\text{aq}}{}^I) \tag{31}$$

$$J_i = k_{\text{L,org}}(C_{i,\text{org}}{}^I - C_{i,\text{org}}) \tag{32}$$

The partition coefficient of HMF and LA between the organic and aqueous phases (m_i) is defined in eq 33 and assumed to be independent of temperature.

$$m_i = \frac{C_{i,\text{org}}{}^I}{C_{i,\text{aq}}{}^I} \tag{33}$$

Combination of eqs 31−33 results in eq 34.

$$J_i \cdot A = \left(C_{i,\text{aq}} - \frac{C_{i,\text{org}}}{m_i}\right) \cdot p \tag{34}$$

where p is the overall mass transfer coefficient as defined in eq 35.

$$p = \frac{A}{\frac{1}{k_{\text{L,aq}}} + \frac{1}{m_i \cdot k_{\text{L,org}}}} \tag{35}$$

The combination of eqs 27−35 leads to the following mole balances for HMF and LA in the aqueous and in the organic phase (eqs 36−39).

$$\frac{dC_{\text{HMF,aq}}}{dt} = R_{1\text{T}} - R_{1\text{H}} - R_{2\text{H}} - \left(C_{\text{HMF,aq}} - \frac{C_{\text{HMF,org}}}{m_{\text{HMF}}}\right) p \tag{36}$$

$$\frac{dC_{\text{HMF,org}}}{dt} = \left(C_{\text{HMF,aq}} - \frac{C_{\text{HMF,org}}}{m_{\text{HMF}}}\right) p \tag{37}$$

$$\frac{dC_{\text{LA,aq}}}{dt} = R_{1\text{H}} - \left(C_{\text{LA,aq}} - \frac{C_{\text{LA,org}}}{m_{\text{LA}}}\right) p \tag{38}$$

$$\frac{dC_{\text{LA,org}}}{dt} = \left(C_{\text{LA,aq}} - \frac{C_{\text{LA,org}}}{m_{\text{LA}}}\right) p \tag{39}$$

A total of 1146 data points (25 batch experiments, 6−10 samples per experiment, with the corresponding concentrations of GAL, TAG, HMF, and LA in both phases for each sample) were used to develop the kinetic model. The kinetic parameters were determined using a nonlinear regression method (lsqnonlin, MATLAB R2020a). The best estimates of the kinetic parameters for the model are shown in Table 5. A comparison between the experimental data and the output of the kinetic model shows a good fit over a broad range of reaction conditions (Figure 11), which is confirmed by a parity plot

Table 5. Estimated Kinetic Parameters for GAL Conversion to HMF in Water/MIBK

parameter	estimated value	parameter	estimated value
$k_{1\text{RG}}$ (M·min^{-1})	0.549 ± 0.022	$E_{1\text{G}}$ (kJ·mol^{-1})	181.5 ± 4.5
$k_{2\text{RG}}$ (M·min^{-1})	0.566 ± 0.030	$E_{2\text{G}}$ (kJ·mol^{-1})	117.9 ± 2.9
$k_{1\text{RT}}$ (M·min^{-1})	0.611 ± 0.042	$E_{1\text{T}}$ (kJ·mol^{-1})	138.8 ± 6.3
$k_{2\text{RT}}$ (M·min^{-1})	0.035 ± 0.025	$E_{2\text{T}}$ (kJ·mol^{-1})	116.5 ± 3.5
$k_{3\text{RT}}$ (M·min^{-1})	1.642 ± 0.049	$E_{3\text{T}}$ (kJ·mol^{-1})	64.2 ± 4.1
$k_{1\text{RH}}$ (M·min^{-1})	0.115 ± 0.027	$E_{1\text{H}}$ (kJ·mol^{-1})	123.5 ± 5.3
$k_{2\text{RH}}$ (M·min^{-1})	0.059 ± 0.038	$E_{2\text{H}}$ (kJ·mol^{-1})	135.6 ± 7.9
p	0.213 ± 0.048	m_{HMF}	0.955 ± 0.062
		m_{LA}	0.539 ± 0.030

(Figure 12). The goodness of fit was assessed by the coefficient of determination (R^2) which was calculated using eq 40.

$$R^2 = 1 - \frac{\sum_{i=1}^{n}(C_i - \hat{C}_i)^2}{\sum_{i=1}^{n}(C_i - \overline{C}_i)^2} \tag{40}$$

where C_i is the experimental concentration of component i, $\hat{C}_i$ is the estimated value of matrix C_i, $\overline{C}_i$ is the average value of matrix C_i, and n is the number of the experimental data.

3.5. Comparison of Model Parameters with the Literature Data. *3.5.1. Activation Energies.* The activation energies for the various reactions have been calculated from the model and can be compared with the literature data. In Figure 13, the activation energies reported in the literature for the conversion of various aldohexoses (GLU, GAL) and ketohexoses (FRC, TAG) are shown, together with the model data from this work. It is difficult to draw general conclusions on the relation between the type of C6-sugar and the activation energy, as the spread in data is considerable. In addition, very limited data are available for TAG. However, the modeled activation energy for TAG dehydration to HMF using the HCl/AlCl$_3$ catalyst system ($E_{1\text{T}} = 138.8 \pm 6.3$ kJ/mol) falls within the range of activation energies for TAG degradation in citrate and phosphate buffer solutions reported by Luecke et al. (131−162 kJ/mol). Still, this value is much larger than the value reported by van Putten (89 ± 15 kJ/mol) (Figure 13).[41,42] However, direct comparison is difficult due to differences in (i) types of catalysts, (ii) solvents (monophase versus biphasic), (iii) the proposed reaction networks used for the kinetic modeling, and (iv) the assumptions made in the kinetic models (e.g., order in substrates).

3.5.2. Kinetics of GAL-TAG Isomerization. Isomerization of GAL to TAG is an important feature in the reaction network and appears to be essential to obtaining high HMF yields. The activation energy of GAL to TAG isomerization was calculated at 117.9 ± 2.9 kJ mol^{-1}. Very limited kinetic data for GAL isomerization to TAG are available in the literature (Figure 14). Murzin et al. reported an activation energy of 99 ± 8 kJ mol^{-1} using a magnesium aluminate catalyst in water,[53] which is close to the value found in our study.

As a comparison, the literature data on the activation energy for GLU isomerization to FRC are also provided in Figure 14 and show a widespread (48−125 kJ mol^{-1}), mainly due to differences in conditions (water versus biphasic solvents and different catalysts). Most of the studies were conducted in aqueous solutions. Only Wang et al.[54] and Tang et al.[47] have utilized a biphasic system with water and an organic solvent (sec-butyl phenol or tetrahydrofuran, respectively). These two studies on the isomerization of GLU to FRC are the most

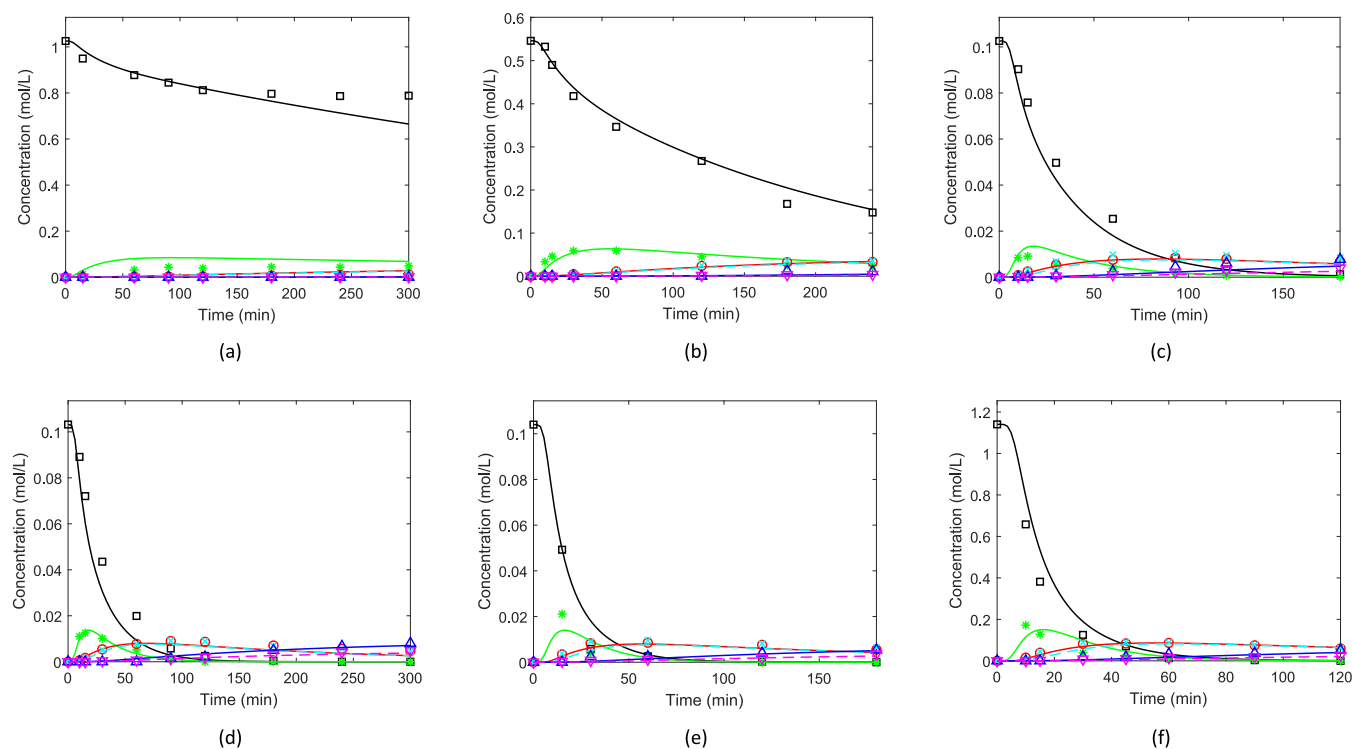**Figure 11.** Comparison of the experimental data (black □: GAL; green *: TAG; red ○: HMF,aq; cyan × : HMF,org; blue △: LA,aq; magenta ▽: LA,org) and kinetic model (solid and dashed lines). Conditions: (a) $T = 112\ °C$; $C_{HCl} = C_{AlCl_3} = 0.08\ M$; $C_{GAL,0} = 1\ M$, (b) $T = 127\ °C$; $C_{HCl} = C_{AlCl_3} = 0.04\ M$; $C_{GAL,0} = 0.5$, (c) $T = 135\ °C$; $C_{HCl} = C_{AlCl_3} = 0.08\ M$; $C_{GAL,0} = 0.1\ M$, (d) $T = 143\ °C$; $C_{HCl} = C_{AlCl_3} = 0.04\ M$; $C_{GAL,0} = 0.1\ M$, (e) $T = 153\ °C$; $C_{HCl} = C_{AlCl_3} = 0.02\ M$; $C_{GAL,0} = 0.1\ M$, (f) $T = 153\ °C$; $C_{HCl} = C_{AlCl_3} = 0.02\ M$; $C_{GAL,0} = 1\ M$.
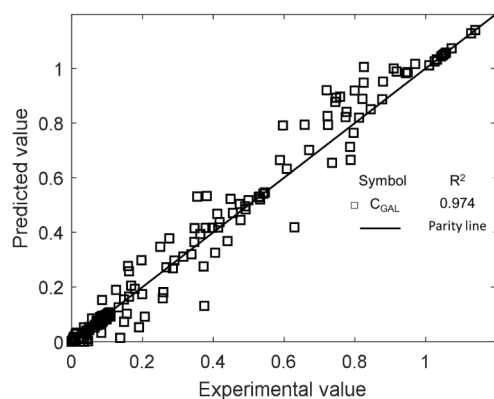

Figure 12. Parity plot for GAL conversion to HMF in the water/MIBK system.

relevant for comparison with our study, as AlCl$_3$ was also used in these studies as the catalyst. The reported E_A values for these studies were 125 kJ mol^{-1}[54] and 95 kJ mol^{-1},[47] respectively. Thus, the E_A value for GAL to TAG isomerization as found by us $(117.9 \pm 2.9\ kJ\ mol^{-1})$ is actually in the same range as the values for GLU-FRC isomerization.

The activation energy for the reaction of GAL to TAG (117.9 $\pm$ 2.9 kJ mol^{-1}) is larger than that of the reverse reaction (TAG to GAL, 64.2 $\pm$ 4.1 kJ mol^{-1}), see Figure 14 for details, indicating that the isomerization reaction is endothermic in nature (vide infra). It would be of interest to compare the modeled activation energy for the reverse reaction (TAG to GAL) with the values reported in the literature. Unfortunately, this information is not available. However, a comparison with the GLU-FRC isomerization system is possible, see Figure 14 for details. Indeed, the

activation energy of the forward reaction (GLU-FRC) is in all cases larger than that of the reverse reaction.[47,58,59]

3.5.3. Thermodynamics of GAL-TAG Isomerization. With the kinetic model available, the equilibrium constant (K_{eq}, eq 41) and the temperature dependence of the equilibrium constant (eq 42) may be calculated for the equilibrium isomerization reaction GAL-TAG. The results are given in Figure 15, left, and show that the K_{eq} increases with temperature, which is indicative of an endothermic reaction. Within the temperature range of this study (385−426 K), the K_{eq} was found to be in the range of 0.10−0.49.

$$K_{eq} = \frac{k_{2G}}{k_{3T}} \tag{41}$$

$$K_{eq} = 3 \times 10^{-8} e^{0.039T} \tag{42}$$

The relation between the standard enthalpy ($\Delta H°$) and entropy ($\Delta S°$) of the isomerization reaction and K_{eq} is given in eq 43.

$$\ln K_{eq} = -\frac{\Delta H°}{RT} + \frac{\Delta S°}{R} \tag{43}$$

A plot of $\ln K_{eq}$ versus $1/T$ is given in Figure 15 (right) and may be represented by eq 44.

$$\ln K_{eq} = -6.4621 \times 10^3 \frac{1}{T} + 14.582 \tag{44}$$

When assuming that $\Delta H°$ and $\Delta S°$ are temperature independent, the GAL-TAG isomerization is thus endothermic with a heat of reaction ($\Delta H°$) of 53.7 kJ mol^{-1}.
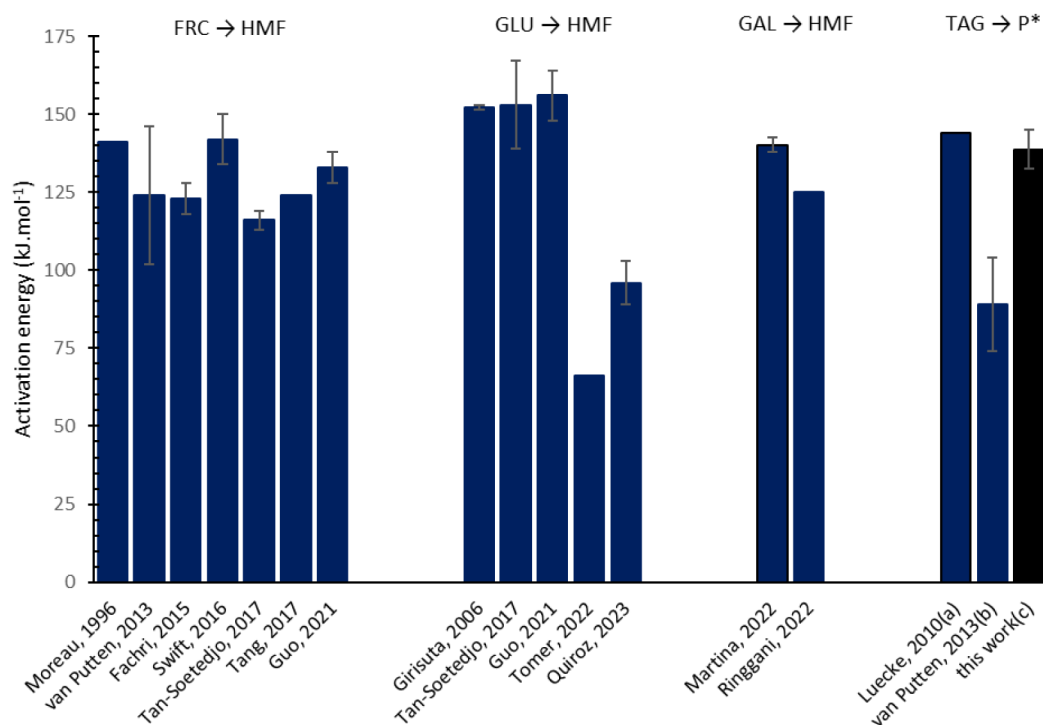
Figure 13. Activation energies for the conversion of C6-sugars to HMF in various catalytic systems.[8,41,50−52,42−49] P* is the degradation/dehydration product of TAG; (a) the degradation/dehydration product is not defined, and the E_A value represents the average E_A value; (b) the degradation/dehydration product is not defined; (c) the degradation/dehydration product is HMF.
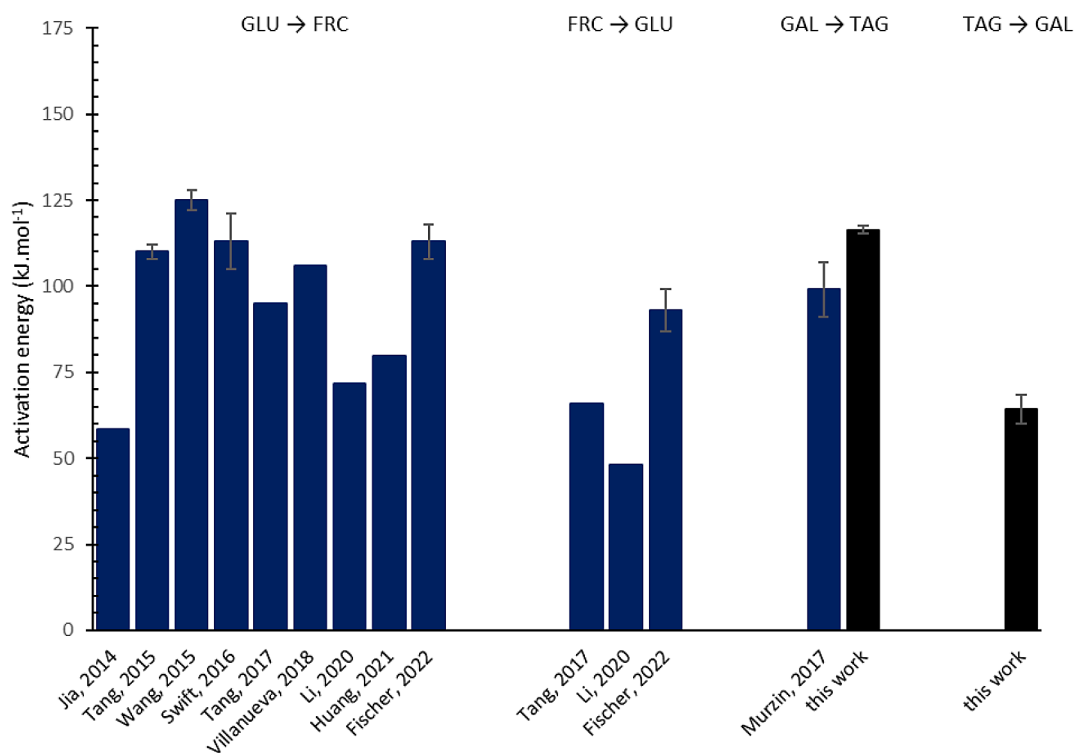

Figure 14. Activation energies reported for the isomerization of GLU to FRC and GAL to TAG using different catalysts in various solvent systems.[45,47,53−59] Additional information is provided in Table S5.

3.5.4. Partitioning Coefficients of HMF and LA. The modeled partition coefficient of HMF (m_{HMF}) for MIBK/water is 0.955 ± 0.062 in the temperature window used in this investigation. This value is slightly higher than that reported by

Guo et al. (0.784−0.916) for the same biphasic system[8] and by Shimanouchi et al. (0.85, 180 °C, MIBK/water).[60]

The modeled LA partition coefficient (m_{LA}) is 0.539 ± 0.030 and is within the same range of values as reported by Datta et al.
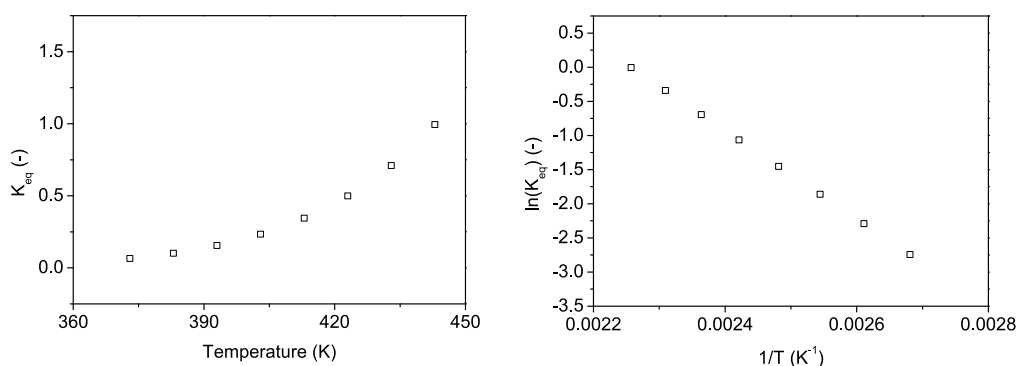
Figure 15. Equilibrium constants (K_{eq}) for the isomerization of GAL to TAG as a function of temperature (left) and the plot of the ln K_{eq} versus the inverse temperature (right).

(0.289–0.697 in MIBK/water and 298 K).[61] Our result is only slightly higher than the value reported by Pereira et al. (0.49 in MIBK/water, 298 and 313 K).[62]

4. INDUSTRIAL SIGNIFICANCE

Rosenfeld et al. have recently published a comprehensive review on the industrial-scale production of HMF. Two key elements were identified to improve techno-economic viability, viz. (i) a cost-effective sugar feed is required, and (ii) HMF separation and purification stand out as one of the biggest challenges during scale-up.[63] When considering challenge 1, many publications have focused on the use of monosaccharides, particularly FRC and GLU as starting materials. In contrast, there are limited reports on the utilization of GAL and the use of biomass feeds, from which GAL can be obtained in a cost-effective manner. Examples of such feeds include macroalgae or seaweed, lactose, and dairy waste. For example, red seaweed contains significant amounts of GAL in the form of agarose and carrageenan and is potentially very attractive for HMF synthesis. When considering challenge 2, the use of a biphasic system for HMF synthesis may have advantages compared with a monophasic one. HMF is extracted into an organic solvent, which facilitates workup as (i) the solution is less acidic as inorganic acids and Al salts are not extracted and remain in the aqueous phase and (ii) the organic phase may be tuned to have a low boiling point. Both will reduce thermal- and acid-catalyzed degradation of HMF during workup. A clear advantage of the use of a biphasic system, besides facilitating workup, is a much higher HMF yield than for a monophasic aqueous system. The current study revealed that GAL conversion to HMF using HCl/AlCl$_3$ as the catalyst and a biphasic reaction system involving both water and MIBK gave a maximum HMF yield of 49 mol % which is much higher than that found for aqueous systems (below 10 mol %).

5. CONCLUSIONS

Our study demonstrates that the use of a biphasic (water/MIBK) system with an HCl/AlCl$_3$ catalyst is a promising method to enhance the HMF yield from GAL. A maximum HMF yield of 49 mol % was obtained whereas a monophasic aqueous system leads to much lower yields (<10 mol %). We have shown that the Lewis acid (AlCl$_3$) plays a pivotal role and effectively catalyzes the isomerization of GAL to TAG. The latter, a ketohexose, is a much better feed for HMF than an aldohexose like GAL. This reaction of TAG toward HMF is catalyzed by HCl, the Brønsted part of the combination catalyst. After HMF is formed, it is extracted into the organic phase where it is more or less protected from further reactions/degradation.

A kinetic model has been developed based on batch reaction data and a proposed reaction network. The agreement between the experimental and modeled data was good. With the kinetic parameters available, the equilibrium constant for the isomerization of GAL to TAG was determined and found to be between 0.10 and 0.49 within the temperature range of this study (385–426 K) with a heat of reaction (ΔH^o) of +53.7 kJ mol^{-1}. These results compare quite well with the (limited) literature data available. The kinetic model can be used as an input for reactor design in future studies to optimize HMF yields. The results allow for efficient reactor selection and design for the conversion of GAL-rich feeds (e.g., red seaweed) to HMF. Currently, these studies are ongoing and will be reported in due course.

■ ASSOCIATED CONTENT

ⓢ **Supporting Information**

The Supporting Information is available free of charge at https://pubs.acs.org/doi/10.1021/acsomega.4c02242.

> Overview of related studies on GAL isomerization to TAG, experimental data series, heat transfer experiments, estimation of the volume change ratio of the aqueous and organic phase, data and model plots of all experimental series, and related studies on GAL and GLU isomerization using various catalysts in water and biphasic systems (PDF)

■ AUTHOR INFORMATION

Corresponding Author

Hero J. Heeres — *Department of Chemical Engineering (ENTEG), University of Groningen, Groningen, AG 9747, The Netherlands;* ⓞ orcid.org/0000-0002-1249-543X; Email: h.j.heeres@rug.nl

Authors

Angela Martina — *Department of Chemical Engineering, Parahyangan Catholic University, Bandung 40141, Indonesia; Department of Chemical Engineering (ENTEG), University of Groningen, Groningen, AG 9747, The Netherlands*

Henk H. van de Bovenkamp — *Department of Chemical Engineering (ENTEG), University of Groningen, Groningen, AG 9747, The Netherlands*

Jozef G. M. Winkelman — *Department of Chemical Engineering (ENTEG), University of Groningen, Groningen, AG 9747, The Netherlands;* ⓞ orcid.org/0000-0001-7888-1731

Inge W. Noordergraaf − *Department of Chemical Engineering (ENTEG), University of Groningen, Groningen, AG 9747, The Netherlands*

Francesco Picchioni − *Department of Chemical Engineering (ENTEG), University of Groningen, Groningen, AG 9747, The Netherlands;* ⊙ orcid.org/0000-0002-8232-2083

Notes

■ ACKNOWLEDGMENTS

■ ABBREVIATIONS

α_{aq}, correction factor for volume of aqueous phase at 20 °C (−); α_{org}, correction factor for volume of organic phase at 20 °C (−); A, interfacial area between the water and organic phases (m^2 L^{-1}); C_{AlCl_3}, concentration of aluminum chloride (M); $C_{AlCl_3,0}$, initial concentration of aluminum chloride (M); $C_{aq,s,0}$, initial concentration of substrate in aqueous phase (M); $C_{aq,p,1}$, concentration of substrate in aqueous phase after reaction (M); C_{GAL}, concentration of GAL (M); $C_{GAL,0}$, initial concentration of GAL (M); $C_{GAL,aq}$, concentration of GAL in aqueous phase (M); C_{HCl}, concentration of hydrochloric acid (M); $C_{HCl,0}$, initial concentration of hydrochloric acid (M); $C_{HCl/AlCl_3}$, concentration of hydrochloric acid and aluminum chloride mixture (M); C_{HMF}, concentration of HMF (M); $C_{HMF,0}$, initial concentration of HMF (M); $C_{HMF,aq}$, concentration of HMF in aqueous phase (M); $C_{HMF,org}$, concentration of HMF in organic phase (M); $C_{i,aq}$, concentration of component i in aqueous phase (M); $C_{i,aq}^I$, concentration of component i at interphase (M); $C_{i,org}$, concentration of component i in organic phase (M); $C_{i,org}^I$, concentration of component i at interphase (M); C_{LA}, concentration of LA (M); $C_{LA,aq}$, concentration of LA in aqueous phase (M); $C_{LA,org}$, concentration of LA in organic phase (M); $C_{org,p,1}$, concentration of component product in organic phase after reaction (M); C_{TAG}, concentration of TAG (M); $C_{TAG,aq}$, concentration of TAG in aqueous phase (M); E_{1G}, activation energy of k_{1G} (kJ mol^{-1}); E_{1H}, activation energy of k_{1H} (kJ mol^{-1}); E_{1T}, activation energy of k_{1T} (kJ mol^{-1}); E_{2G}, activation energy of k_{2G} (kJ mol^{-1}); E_{2H}, activation energy of k_{2H} (kJ mol^{-1}); E_{2T}, activation energy of k_{2T} (kJ mol^{-1}); E_{3T}, activation energy of k_{3T} (kJ mol^{-1}); γ_{aq}, correction factor for volume of aqueous phase at reaction temperature (−); γ_{org}, correction factor for volume of organic phase reaction temperature (−); J_i, molar mass transfer rate of component i (mol min^{-1} m^{-2}); k_{1G}, reaction rate constant of GAL for the side reaction to humins (min^{-1}); k_{1RG}, reaction rate constant k_{1G} at reference temperature (min^{-1}); k_{1H}, reaction rate constant of HMF for the main reaction (min^{-1}); k_{1RH}, reaction rate constant k_{1H} at reference temperature (min^{-1}); k_{1T}, reaction rate constant of TAG for the main reaction (min^{-1}); k_{1RT}, reaction rate constant k_{1T} at reference temperature (min^{-1}); k_{2G}, reaction rate constant of GAL for the isomerization reaction (min^{-1}); k_{2RG}, reaction rate constant k_{2G} at reference temperature (min^{-1}); k_{2H}, reaction rate constant of HMF for the side reaction to humins (min^{-1}); k_{2RH}, reaction rate constant k_{2H} at reference temperature (min^{-1}); k_{2T}, reaction rate constant of TAG for the side reaction to humins (min^{-1}); k_{2RT}, reaction rate constant k_{2T} at reference temperature (min^{-1}); k_{3T}, reaction rate constant of TAG for the isomerization reaction (min^{-1}); k_{3RT}, reaction rate constant k_{3T} at reference temperature (min^{-1}); K_{eq}, equilibrium constant for the isomerization reaction (−); $k_{L,aq}$, local mass transfer coefficient in aqueous phase (min^{-1}); $k_{L,org}$, local mass transfer coefficient in organic phase (min^{-1}); m_i, partition coefficient of component i (−); R, gas constant (kJ mol^{-1} K^{-1}); R_{1G}, reaction rate of GAL conversion to humins (M min^{-1}); R_{1H}, reaction rate of HMF conversion to LA and FA (M min^{-1}); R_{1T}, reaction rate of TAG conversion to HMF (M min^{-1}); R_{2G}, reaction rate of GAL isomerization to TAG (M min^{-1}); R_{2H}, reaction rate of HMF conversion to humins (M min^{-1}); R_{2T}, reaction rate of TAG conversion to humins (M min^{-1}); R_{3T}, reaction rate of TAG isomerization to GAL (M min^{-1})); t, reaction time (min); T, reaction temperature (°C); T_R, reference temperature (°C); V_{aq}, volume of aqueous phase (mL); $V_{aq,0}$, initial volume of aqueous phase (mL); $V_{aq,1}$, volume of aqueous phase after reaction time (mL); $V_{org,0}$, initial volume of organic phase (mL); $V_{org,1}$, volume of organic phase after reaction time (mL); X_s, conversion of substrate (mol %); Y_p, yield of products (mol %); $\Delta G°$, standard free energy change (kJ mol^{-1}); $\Delta H°$, standard enthalpy change (kJ mol^{-1}); $\Delta S°$, standard entropy change (kJ mol^{-1} K^{-1})

■ REFERENCES

(1) Signoretto, M.; Taghavi, S.; Ghedini, E.; Menegazzo, F. Catalytic Production of Levulinic Acid (LA) from Actual Biomass. *Molecules* **2019**, *24* (15), 2760.

(2) Van Putten, R. J.; Van Der Waal, J. C.; De Jong, E.; Rasrendra, C. B.; Heeres, H. J.; De Vries, J. G. Hydroxymethylfurfural, a Versatile Platform Chemical Made from Renewable Resources. *Chem. Rev.* **2013**, *113* (3), 1499−1597.

(3) de Jong, E.; Stichnothe, H.; Bell, G.; Jorgensen, H. *Bio-Based Chemicals: A 2020 Update*; IEA Bioenergy, 2020.

(4) Esteban, J.; Vorholt, A. J.; Leitner, W. An Overview of the Biphasic Dehydration of Sugars to 5-Hydroxymethylfurfural and Furfural: A Rational Selection of Solvents Using COSMO-RS and Selection Guides. *Green Chem.* **2020**, *22* (7), 2097−2128.

(5) Soukup-Carne, D.; Fan, X.; Esteban, J. An Overview and Analysis of the Thermodynamic and Kinetic Models Used in the Production of 5-Hydroxymethylfurfural and Furfural. *Chem. Eng. J.* **2022**, *442* (P2), 136313.

(6) Abdul Rani, M. A. A. B.; Karim, N. A.; Kamarudin, S. K. Recent Reaction Systems for the Synthesis of 5-Hydroxymethylfurfural (HMF) from Carbohydrates with Process Development Analysis: A Review. *Int. J. Energy Res.* **2022**, *46* (13), 18996−19050.

(7) Jia, S.; He, Y.; Wang, G. Dimethylsulfoxide/Water Mixed Solvent Mediated Synthesis of 5-Hydroxymethylfurfural from Galactose with Aluminum Salt Catalyst. *ChemistrySelect.* **2017**, *2* (8), 2356−2362.

(8) Guo, W.; Zhang, Z.; Hacking, J.; Heeres, H. J.; Yue, J. Selective Fructose Dehydration to 5-Hydroxymethylfurfural from a Fructose-Glucose Mixture over a Sulfuric Acid Catalyst in a Biphasic System: Experimental Study and Kinetic Modelling. *Chem. Eng. J.* **2021**, *409* (November 2020), 128182.

(9) Rigal, L.; Gaset, A. Direct Preparation of 5-Hydroxymethyl-2-Furancarboxaldehyde from Polyholosides: A Chemical Valorisation of the Jerusalem Artichoke (Helianthus Tuberosus L.). *Biomass* **1983**, *3* (2), 151−163.

(10) Guo, W.; Heeres, H. J.; Yue, J. Continuous Synthesis of 5-Hydroxymethylfurfural from Glucose Using a Combination of AlCl3 and HCl as Catalyst in a Biphasic Slug Flow Capillary Microreactor. *Chem. Eng. J.* **2020**, *381* (June 2019), 122754.

(11) van Putten, R. J.; van der Waal, J. C.; de Jong, E.; Heeres, H. J. Reactivity Studies in Water on the Acid-Catalysed Dehydration of Psicose Compared to Other Ketohexoses into 5-Hydroxymethylfurfural. *Carbohydr. Res.* **2017**, *446−447*, 1−6.

(12) Drabo, P.; Delidovich, I. Catalytic Isomerization of Galactose into Tagatose in the Presence of Bases and Lewis Acids. *Catal. Commun.* **2018**, *107* (November2017), 24−28.

(13) Dijkmans, J.; Gabriëls, D.; Dusselier, M.; De Clippel, F.; Vanelderen, P.; Houthoofd, K.; Malfliet, A.; Pontikes, Y.; Sels, B. F. Productive Sugar Isomerization with Highly Active Sn in Dealuminated *β* Zeolites. *Green Chem.* **2013**, *15* (10), 2777−2785.

(14) Jeong, G. T.; Park, D. H. Production of Sugars and Levulinic Acid from Marine Biomass Gelidium Amansii. *Appl. Biochem. Biotechnol.* **2010**, *161* (1−8), 41−52.

(15) Meinita, M. D. N.; Hong, Y. K.; Jeong, G. T. Comparison of Sulfuric and Hydrochloric Acids as Catalysts in Hydrolysis of Kappaphycus Alvarezii (Cottonii). *Bioprocess Biosyst. Eng.* **2012**, *35* (1−2), 123−128.

(16) Meinita, M. D. N.; Marhaeni, B.; Winanto, T.; Setyaningsih, D.; Hong, Y. K. Catalytic Efficiency of Sulfuric and Hydrochloric Acids for the Hydrolysis of Gelidium Latifolium (Gelidiales, Rhodophyta) in Bioethanol Production. *J. Ind. Eng. Chem.* **2015**, *27*, 108−114.

(17) Jeong, G. T.; Ra, C. H.; Hong, Y. K.; Kim, J. K.; Kong, I. S.; Kim, S. K.; Park, D. H. Conversion of Red-Algae Gracilaria Verrucosa to Sugars, Levulinic Acid and 5-Hydroxymethylfurfural. *Bioprocess Biosyst. Eng.* **2015**, *38* (2), 207−217.

(18) Lee, S. B.; Kim, S. K.; Hong, Y. K.; Jeong, G. T. Optimization of the Production of Platform Chemicals and Sugars from the Red Macroalga, Kappaphycus Alvarezii. *Algal Res.* **2016**, *13*, 303−310.

(19) Malihan, L. B.; Mittal, N.; Nisola, G. M.; Weldemhret, T. G.; Kim, H.; Chung, W. J. Macroalgal Biomass Hydrolysis Using Dicationic Acidic Ionic Liquids. *J. Chem. Technol. Biotechnol.* **2017**, *92* (6), 1290−1297.

(20) Park, M.−R.; Kim, S.−K.; Jeong, G.−T. Optimization of the Levulinic Acid Production from the Red Macroalga, Gracilaria Verrucosa Using Methanesulfonic Acid. *Algal Res.* **2018**, *31*, 116−121.

(21) Nunraksa, N.; Rattanasansri, S.; Praiboon, J.; Chirapart, A. Proximate Composition and the Production of Fermentable Sugars, Levulinic Acid, and HMF from Gracilaria Fisheri and Gracilaria Tenuistipitata Cultivated in Earthen Ponds. *J. Appl. Phycol.* **2019**, *31* (1), 683−690.

(22) Bodachivskyi, I.; Kuzhiumparambil, U.; Williams, D. B. G. The Role of the Molecular Formula of ZnCl2·: N H2O on Its Catalyst Activity: A Systematic Study of Zinc Chloride Hydrates in the Catalytic Valorisation of Cellulosic Biomass. *Catal. Sci. Technol.* **2019**, *9* (17), 4693−4701.

(23) Bodachivskyi, I.; Kuzhiumparambil, U.; Williams, D. B. G. Catalytic Valorization of Native Biomass in a Deep Eutectic Solvent: A Systematic Approach toward High-Yielding Reactions of Polysaccharides. *ACS Sustainable Chem. Eng.* **2020**, *8* (1), 678−685.

(24) Chen, Y.; Zhou, Y.; Zhang, R.; Hu, C. Conversion of Saccharides in Enteromorpha Prolifera to Furfurals in the Presence of FeCl3. *Mol. Catal.* **2020**, *484*, 110729.

(25) Zhou, Y.; Li, M.; Chen, Y.; Hu, C. Conversion of Polysaccharides in Ulva Prolifera to Valuable Chemicals in the Presence of Formic Acid. *J. Appl. Phycol.* **2021**, *33* (1), 101−110.

(26) Pereira, A. P.; Woodman, T. J.; Chuck, C. J. An Integrated Biorefinery to Produce 5-(Hydroxymethyl)Furfural and Alternative Fuel Precursors from Macroalgae and Spent Coffee Grounds. *Sustain. Energy Fuels.* **2021**, *5* (23), 6189−6196.

(27) Mondal, D.; Sharma, M.; Maiti, P.; Prasad, K.; Meena, R.; Siddhanta, A. K.; Bhatt, P.; Ijardar, S.; Mohandas, V. P.; Ghosh, A.; et al. Fuel Intermediates, Agricultural Nutrients and Pure Water from Kappaphycus Alvarezii Seaweed. *RSC Adv.* **2013**, *3* (39), 17989−17997.

(28) Kim, J. A.; Lee, S. B. Production of 3,6-Anhydro-D-Galactose from *κ*-Carrageenan Using Acid Catalysts. *Biotechnol. Bioprocess Eng.* **2016**, *21*, 79−86.

(29) Fachri, B. A. Exploratory Study on Thermal Microwave-Assisted Decomposition of Eucheuma Cottonii Carrageenan to 5-Hydroxymethylfurfural and Levulinic Acid in Aqueous Medium. *AIP Conf Proc.* **2018**, *2026*, 020030.

(30) Wagh, A. S.; Ukarde, T. M.; Pandey, P. H.; Lali, A. M.; Pawar, H. S. Self-Catalyzed Deconstruction of Acid-Modified k-Carrageenan for Production of 5-Hydroxymethyl Furfural. *ACS Sustainable Chem. Eng.* **2019**, *7* (16), 13932−13940.

(31) Yan, L.; Laskar, D. D.; Lee, S. J.; Yang, B. Aqueous Phase Catalytic Conversion of Agarose to 5-Hydroxymethylfurfural by Metal Chlorides. *RSC Adv.* **2013**, *3* (46), 24090−24098.

(32) Oh, S. J.; Park, J.; Na, J. G.; Oh, Y. K.; Chang, Y. K. Production of 5-Hydroxymethylfurfural from Agarose by Using a Solid Acid Catalyst in Dimethyl Sulfoxide. *RSC Adv.* **2015**, *5* (59), 47983−47989.

(33) Francavilla, M.; Intini, S.; Luchetti, L.; Luque, R. Tunable Microwave-Assisted Aqueous Conversion of Seaweed-Derived Agarose for the Selective Production of 5-Hydroxymethyl Furfural/Levulinic Acid. *Green Chem.* **2016**, *18* (22), 5971−5977.

(34) Seri, K. I.; Inoue, Y.; Ishida, H. Highly Efficient Catalytic Activity of Lanthanide(III) Ions for Conversion of Saccharides to 5-Hydroxymethyl-2-Furfural in Organic Solvents. *Chem. Lett.* **2000**, *29*, 22−3.

(35) Binder, J. B.; Cefali, A. V.; Blank, J. J.; Raines, R. T. Mechanistic Insights on the Conversion of Sugars into 5- Hydroxymethylfurfural. *Energy Environ. Sci.* **2010**, *3* (6), 765−771.

(36) Tuteja, J.; Nishimura, S.; Ebitani, K. One-Pot Synthesis of Furans from Various Saccharides. *Bull. Chem. Soc. Jpn.* **2012**, *85* (3), 275−281.

(37) Hu, X.; Wu, L.; Wang, Y.; Song, Y.; Mourant, D.; Gunawan, R.; Gholizadeh, M.; Li, C. Z. Acid-Catalyzed Conversion of Mono- and Poly-Sugars into Platform Chemicals: Effects of Molecular Structure of Sugar Substrate. *Bioresour. Technol.* **2013**, *133*, 469−474.

(38) Shi, J.; Liu, W.; Wang, N.; Yang, Y.; Wang, H. Production of 5-Hydroxymethylfurfural from Monoand Disaccharides in the Presence of Ionic Liquids. *Catal. Lett.* **2014**, *144* (2), 252−260.

(39) Flannelly, T.; Lopes, M.; Kupiainen, L.; Dooley, S.; Leahy, J. J. Non-Stoichiometric Formation of Formic and Levulinic Acids from the Hydrolysis of Biomass Derived Hexose Carbohydrates. *RSC Adv.* **2016**, *6* (7), 5797−5804.

(40) Zhao, J.; Wang, Z.; Jin, Q.; Feng, D.; Lee, J. Isomerization of Galactose to Tagatose: Recent Advances in Non-Enzymatic Isomerization. *J. Agric. Food Chem.* **2023**, *71* (10), 4228−4234.

(41) Van Putten, R. J.; Soetedjo, J. N. M.; Pidko, E. A.; Van Der Waal, J. C.; Hensen, E. J. M.; De Jong, E.; Heeres, H. J. Dehydration of Different Ketoses and Aldoses to 5-Hydroxymethylfurfural. *ChemSuschem.* **2013**, *6* (9), 1681−1687.

(42) Luecke, K. J.; Bell, L. N. Thermal Stability of Tagatose in Solution. *J. Food Sci.* **2010**, *75*, C346−C351.

(43) Moreau, C.; Durand, R.; Razigade, S.; Duhamet, J.; Faugeras, P.; Rivalier, P.; Pierre, R.; Avignon, G. Dehydration of Fructose to 5-Hydroxymethylfurfural over H-Mordenites. *Appl. Catal., A.* **1996**, *145* (1−2), 211−224.

(44) Fachri, B. A.; Abdilla, R. M.; Bovenkamp, H. H. V. D.; Rasrendra, C. B.; Heeres, H. J. Experimental and Kinetic Modeling Studies on the Sulfuric Acid Catalyzed Conversion of d -Fructose to 5-Hydroxymethylfurfural and Levulinic Acid in Water. *ACS Sustainable Chem. Eng.* **2015**, *3* (12), 3024−3034.

(45) Swift, T. D.; Nguyen, H.; Erdman, Z.; Kruger, J. S.; Nikolakis, V.; Vlachos, D. G. Tandem Lewis Acid/Brønsted Acid-Catalyzed Conversion of Carbohydrates to 5-Hydroxymethylfurfural Using Zeolite Beta. *J. Catal.* **2016**, *333*, 149−161.

(46) Tan-Soetedjo, J. N. M.; Van De Bovenkamp, H. H.; Abdilla, R. M.; Rasrendra, C. B.; Van Ginkel, J.; Heeres, H. J. Experimental and Kinetic Modeling Studies on the Conversion of Sucrose to Levulinic Acid and 5-Hydroxymethylfurfural Using Sulfuric Acid in Water. *Ind. Eng. Chem. Res.* **2017**, *56* (45), 13228−13239.

(47) Tang, J.; Zhu, L.; Fu, X.; Dai, J.; Guo, X.; Hu, C. Insights into the Kinetics and Reaction Network of Aluminum Chloride-Catalyzed Conversion of Glucose in NaCl-H2O/THF Biphasic System. *ACS Catal.* **2017**, *7* (1), 256−266.

(48) Girisuta, B.; Janssen, L. P. B. M.; Heeres, H. J. Green Chemicals: A Kinetic Study on the Conversion of Glucose to Levulinic Acid. *Chem. Eng. Res. Des.* **2006**, *84* (5), 339−349.

(49) Tomer, R.; Biswas, P. Reaction Kinetics Study and the Estimation of Thermodynamic Parameters for the Conversion of Glucose to 5-Hydroxymethylfurfural (5-HMF) in a Dimethyl Sulfoxide (DMSO) Medium in the Presence of a Mesoporous TiO2 Catalyst. *J. Taiwan Inst. Chem. Eng.* **2022**, *136*, 104427.

(50) Quiroz, N. R.; Chen, T.-H.; Caratzoulas, S.; Vlachos, D. G. Direct Brønsted Acid-Catalyzed Dehydration of Glucose to HMF in Methyl Isobutyl Ketone. *ACS Catal.* **2023**, *13*, 14221−14232.

(51) Martina, A.; Van De Bovenkamp, H. H.; Noordergraaf, I. W.; Winkelman, J. G. M.; Picchioni, F.; Heeres, H. J. Kinetic Study on the Sulfuric Acid-Catalyzed Conversion of d -Galactose to Levulinic Acid in Water. *Ind. Eng. Chem. Res.* **2022**, *61* (26), 9178−9191.

(52) Ringgani, R.; Azis, M. M.; Rochmadi, R.; Budiman, A. Experimental and Kinetic Modeling of Galactose Valorization to Levulinic Acid. *Bull. Chem. React. Eng. Catal.* **2022**, *17* (2), 451−465.

(53) Murzin, D. Y.; Murzina, E. V.; Aho, A.; Kazakova, M. A.; Selyutin, A. G.; Kubicka, D.; Kuznetsov, V. L.; Simakova, I. L. Aldose to Ketose Interconversion: Galactose and Arabinose Isomerization over Heterogeneous Catalysts. *Catal. Sci. Technol.* **2017**, *7* (22), 5321−5331.

(54) Wang, T.; Glasper, J. A.; Shanks, B. H. Kinetics of Glucose Dehydration Catalyzed by Homogeneous Lewis Acidic Metal Salts in Water. *Appl. Catal. A Gen.* **2015**, *498*, 214−221.

(55) Jia, S.; Liu, K.; Xu, Z.; Yan, P.; Xu, W.; Liu, X.; Zhang, Z. C. Reaction Media Dominated Product Selectivity in the Isomerization of Glucose by Chromium Trichloride: From Aqueous to Non-Aqueous Systems. *Catal. Today* **2014**, *234*, 83−90.

(56) Tang, J.; Guo, X.; Zhu, L.; Hu, C. Mechanistic Study of Glucose-to-Fructose Isomerization in Water Catalyzed by $[Al(OH)_2(Aq)]^+$. *ACS Catal.* **2015**, *5* (9), 5097−5103.

(57) Huang, H.; Meng, X. G.; Yu, W. W.; Chen, L. Y.; Wu, Y. Y. High Selective Isomerization of Glucose to Fructose Catalyzed by Amidoximed Polyacrylonitrile. *ACS Omega* **2021**, *6* (30), 19860−19866.

(58) Fischer, M.; Drabo, P.; Delidovich, I. Study of Base-Catalyzed Isomerization of d-Glucose with a Focus on Reaction Kinetics. *React. Kinet., Mech. Catal.* **2022**, *135* (5), 2357−2377.

(59) Li, C.; Wang, Y.; Zhang, Y.; Wang, M.; Sun, X.; Cui, H.; Xie, Y. Isomerization Kinetics of Glucose to Fructose in Aqueous Solution with Magnesium-Aluminum Hydrotalcites. *ChemistrySelect* **2020**, *5* (1), 270−279.

(60) Shimanouchi, T.; Tanifuji, T.; Fujioka, S.; Terasaka, K.; Kimura, Y. Water/Methyl Isobutyl Ketone (MIBK) Biphasic System in Slug Flow under High Temperature and Pressure Conditions. *Solvent Extr. Res. Dev.* **2014**, *21* (2), 201−209.

(61) Datta, D.; Marti, M. E.; Pal, D.; Kumar, S. Equilibrium Study on the Extraction of Levulinic Acid from Aqueous Solution with Aliquat 336 Dissolved in Different Diluents: Solvent's Polarity Effect and Column Design. *J. Chem. Eng. Data.* **2017**, *62* (1), 3−10.

(62) Pereira Santana, M. D.; Belém Lavrador, R. Solvent Screening for Liquid-Liquid Extraction of Levulinic Acid from Aqueous Medium. *Sep. Sci. Technol.* **2022**, *57* (10), 1575−1584.

(63) Rosenfeld, C.; Konnerth, J.; Sailer-Kronlachner, W.; Solt, P.; Rosenau, T.; van Herwijnen, H. W. G. Current Situation of the Challenging Scale-Up Development of Hydroxymethylfurfural Production. *ChemSuschem* **2020**, *13*, 3544−3564.